GEOCHEMISTRY

INTRODUCTION

Over two hundred samples of the Lushs Bight Group including lavas, sheeted diabase dykes, and diabase and gabbro intrusives (dykes and sills) were collected for analysis during the course of this study. (See **Maps 94-227 and 94-229** for sample locations.) Representative samples of all rock types were then chosen on the basis of their chemical characteristics as defined by Ti and Zr discriminate diagrams for further detailed and precise analysis. These representative samples were further complemented by detailed sampling undertaken to clarify stratigraphic and structural relationships. A subset of 93 samples was then chosen for additional analyses—43 samples (Tables 3 and 4) were analyzed for a suite of 28 trace elements by inductively-coupled-plasma—mass-spectrometry (ICP-MS) (Jenner *et al.*, 1990), and 50 samples were analyzed for rare-earth elements (REE) by thin film-x-ray fluorescence (TF-XRF). For these later samples, Th was determined by an element specific ICP-MS routine. Based on these analyses, the Lushs Bight Group was divided into a number of geochemical groups or types.

The ICP-MS data and the average compositions of the geochemical groups within the Lushs Bight Group are presented within this chapter (Tables 3, 4 and 5) for quick reference. The averages incorporate both TF-XRF and ICP-MS data. Eleven Sm—Nd isotopic analysis were also done (Table 6).

Twenty-nine samples from the Western Arm, Cutwell and Catchers Pond groups and 14 samples from the Cooper's Cove and Colchester plutons were also analyzed and are presented here for comparison purposes; 32 volcanic and intrusive rocks of unassigned status were also analyzed. Complete datasets for all the rocks analysed are presented in Appendix 2. The reader is referred to Appendix 3 for sampling and analytical methods, statistics and a discussion of what methods were used on which samples.

ALTERATION

Discussion

The geology, metallogeny and geochemistry of the Lushs Bight Group have generally lead to the interpretation of its formation as oceanic crust; however, the exact tectonic environment of its formation has been debatable (Smitheringale, 1973; Strong, 1977; Kean, 1983, 1984; Jenner *et al.*, 1988). The presence of well-developed sheeted dykes clearly indicates an extensional environment similar to that known or postulated to exist at major ocean-basin spreading ridges, back-arc basins and supra- subduction zone environments. Heat flow, mineralogic and isotopic studies of the ocean floor (e.g., Lister 1974) show that seawater circulates through oceanic crust to depths of at least several kilometres and is chemically transformed through reaction with rocks and attain temperatures up to 400 to 500°C. Discharge of hydrothermal fluids circulating in oceanic crust, both at major ocean ridges and back-arc basins, occurs in submarine hot springs (also described as black or white smokers) (e.g., Mottl, 1983). Significant changes in the mineralogy and geochemistry of the oceanic crust accompanies the circulation of seawater (e.g.,

Humphris and Thompson, 1978a, b). In order to use the geochemistry of ancient volcanic rocks to establish their paleotectonic setting and petrogenetic relationships, it is necessary to establish which element concentrations and/or element ratios have remained unaffected (immobile) or at least still record the original relative abundance patterns.

There are a number of approaches by which the relative mobility of elements can be ascertained, including comparative studies of fresh versus altered portions of individual samples (Bienvenu *et al.*, 1990), comparison of populations of altered versus fresh samples, establishing mobility vectors by comparing altered versus more altered portions of individual flows (e.g., core vs rim variations in pillow lavas) (Humphries and Thompson, 1978a, b), consideration of variation diagrams and element-ratio plots to determine if coherent and/or predictable igneous geochemical behaviour is observed (Arndt and Jenner, 1986), experimental studies of basalt—seawater interaction (Seyfried and Mottl, 1982; Hajash, 1984), and analyses of hydrothermal fluids (Michard and Albarede, 1986).

The variables that control the nature of alteration, and therefore element mobility, are: temperature, pressure, relative abundance and nature of primary and secondary phases, textural characteristics of the rock (e.g., degree of crystallinity), permeability, and fluid/rock mass ratio (Mottl and Seyfried, 1980). It is difficult to identify a single variable as being most important; for example, the fluid/rock mass ratio, that according to Mottl and Seyfried (1980) is arguably the most important variable, depends on factors such as "relative rates of fluid flow versus reaction in that locality, which in turn depend on such factors as permeability, surface area, temperature, and type of rock being altered."

The fluid/rock (F/R) mass ratio has a marked effect on chemistry of the hydrothermal solution, the mineralogy of the solids produced and the mobility of elements. Under the conditions that are appropriate for submarine, sub-seafloor alteration, two hydrothermal systems can be defined based on the fluid/rock ratio: rock-dominated hydrothermal system (RDHS) and seawater-dominated hydrothermal system (SWDHS). Mottl and Seyfried (1980) showed that the transition between RDHS and SWDHS occurs in experimental seawater - basalt interaction experiments at a fluid/rock ratio of 50 ± 5 (see Figure 6). The transition between the two systems observed in the experiments is quite abrupt and apparently temperature independent, at least up to about 400 C. The fundamental difference between RDHS and SWDHS results from the role of seawater Mg+ in generating and maintaining acidity in the hydrothermal solution (Mottl and Seyfried, 1980; Seyfried, 1987). During seawater—basalt interaction, two types of reactions compete to control pH: reactions removing seawater Mg and generating H+; and silicate hydrolysis reactions generating cations and consuming H+.

In RDHS (F/R < 50) the Mg in seawater is effectively removed and is fixed in the rocks by formation of Mg-rich secondary mineral phases. At low to moderate temperatures (150 to 350 C), Ca replaces Mg, and at very low F/R ratios Na and K replaces Mg; however, at temperatures > 350 C, Ca and Na tend to be fixed in solid phases. The acid-generating stage of alteration in this system is thus relatively early and brief. With the elimination of Mg from the hydrothermal solution, and the resulting neutralization of the solution acidity, the leaching of base and heavy metals ceases. Sodium-metasomatism is dominant in rock-dominated hydrothermal systems that are relatively SiO2-rich; whereas, Ca-metasomatism dominates systems that are relatively SiO2-poor (Seyfried, 1987). Typical minerals or mineral assemblages thought to be produced in natural basaltic rocks by a rock-dominated hydrothermal system are smectites, zeolites, prehnite, albite, saponite, actinolitic amphibole, chlorite, epidote, quartz, sphene and pyrite (see Figure 6) (Seyfried, 1987; Mottl and Seyfried, 1980). There are some elements in the basalts that will be effectively partitioned into the fluid phase because there are no sites available (or preferable) to them in the alteration assemblages. These so-called soluble elements include Cl, Br, B, Cs, F, Li, and As; K and Ba may also behave in a similar manner.

In SWDHS (F/R > 50) removal of the Mg from seawater is incomplete, because in this fluid-dominated system there are insufficient cations available from the altering basalt to exchange with Mg. Under these conditions, H+ production is prolonged and the hydrothermal solution is always acidic, which leads to the breakdown of all but the most acid-resistant minerals. The dominant alteration products are chlorite, chlorite— smectite and quartz. Under these conditions base and heavy metals are effectively leached from the rock; Fe is leached from the rock at high temperatures. In SWDHS (because of the acidity and simple alteration mineralogy), several more elements can be added to the list of soluble elements, including K, Ba, Cu, Ca, Na, Mn and Zn (± Fe).

Natural systems are open and isothermal and two important factors apply to them (Mottl and Seyfried, 1980):

1) rock-dominated and seawater-dominated systems can exist at the same time in different localities, and in the same place at different times—depending on locally controlled factors; and,

2) most hydrothermal systems operative during alteration of oceanic crust are rock-dominated. SWDHS are

Table 3. Composition of Lushs Bight Group lavas (ICP-MS). Each geochemical type is listed by decreasing Mg#

Column	1	2	3	4	5	6	7	8	9	10	11	12	13	14
Sample #	1543328	1543329	1543365	1543334	1543366	1543335	1543337	1543336	1542118	1543347	1542129	1542263	1543326	1542119
Group	BON	BON	BON	BON	BON	BON	BON	BON	BON	BON	LOTI	LOTI	IAT-II	IAT-II
SiO_2	57.5	55.0	56.6	55.7	63.0	59.1	56.8	62.9	54.8	54.7	53.36	51.14	56.4	52.6
TiO_2	0.1	0.1	0.1	0.1	0.2	0.2	0.1	0.1	0.2	0.2	0.39	0.62	0.9	0.8
Al_2O_3	8.5	8.3	11.4	13.3	12.5	12.8	12.1	10.1	14.6	14.4	15.94	15.85	15.6	17.0
FeO*	8.1	9.5	7.7	9.0	6.2	7.4	8.8	7.7	7.8	8.7	6.93	10.61	7.8	9.4
MnO	0.2	0.2	0.2	0.1	0.1	0.1	0.2	0.2	0.1	0.2	0.15	0.17	0.1	0.2
MgO	15.6	17.9	12.3	12.5	8.0	9.4	10.3	8.8	8.1	6.8	5.49	7.67	7.9	9.3
CaO	7.9	7.9	10.1	6.0	5.2	5.5	7.2	6.2	13.2	11.9	17.40	10.41	4.8	6.5
Na_2O	0.5	0.2	1.5	1.7	4.7	5.4	4.0	3.8	1.1	3.1	0.30	2.93	6.2	4.2
K_2O	1.56	1.00	0.12	1.50	0.09	0.10	0.40	0.20	0.13	0.09	0.03	0.31	0.33	0.05
P_2O_5	0.01	0.01	0.02	0.01	0.00	0.01	0.03	0.02	0.01	0.02	0.01	0.04	0.05	0.04
Mg#	77	77	74	71	70	69	68	67	65	58	58	57	64	64
LOI	4.7	4.6	2.9	4.5	1.9	2.6	2.4	1.9	2.4	1.7	2.54	2.66	3.0	3.1
Cr	988	1179	1058	527	485	325	838	955	419	380	157	84	308	179
Ni	205	249	305	80	81	73	176	195	82	81	60	42	122	65
V	208	234	247	260	243	274	264	254	253	253	202	335	259	329
Nb	0.9	0.7	1.1	1.3	1.0	0.9	0.8	0.8	0.9	0.9	0.5	0.4	0.8	0.7
Zr	18	19	24	20	17	22	20	22	17	35	16	33	39	30
Y	4	3	3	4	5	5	2	2	5	5	10	18	18	18
Th	0.44	0.40	0.30	0.54	0.42	0.32	0.25	0.24	0.32	0.57	0.17	0.25	0.20	0.18
La	1.91	1.19	1.31	1.19	1.79	1.30	0.52	0.73	1.14	1.76	0.88	1.80	0.89	1.23
Ce	3.51	2.42	2.69	2.87	3.37	3.07	1.47	1.62	2.50	3.67	1.72	4.02	3.11	3.87
Pr	0.41	0.27	0.33	0.36	0.41	0.41	0.16	0.20	0.29	0.44			0.65	0.65
Nd	1.40	1.12	1.27	1.52	1.68	1.79	0.65	0.88	1.31	1.84	1.72	4.55	4.00	3.91
Sm	0.44	0.32	0.28	0.48	0.52	0.58	0.31	0.24	0.32	0.56	0.91	1.48	1.75	1.53
Eu	0.13	0.08	0.09	0.13	0.14	0.16	0.07	0.08	0.18	0.20	0.54	1.01	0.60	0.62
Gd	0.34	0.28	0.35	0.36	0.49	0.57	0.19	0.20	0.56	0.64	0.97	2.86	2.46	2.25
Tb	0.07	0.06	0.06	0.11	0.11	0.11	0.03	0.04	0.10	0.10		0.00	0.49	0.44
Dy	0.53	0.43	0.49	0.64	0.92	0.87	0.29	0.35	0.83	0.76	1.40	3.70	3.38	3.12
Ho	0.13	0.11	0.10	0.14	0.22	0.20	0.07	0.07	0.20	0.20			0.76	0.72
Er	0.48	0.40	0.40	0.56	0.77	0.60	0.23	0.27	0.67	0.65	1.40	1.58	2.20	2.03
Tm	0.08	0.07	0.06	0.09	0.11	0.10	0.04	0.05	0.09	0.11			0.31	0.30
Yb	0.59	0.54	0.59	0.90	0.89	0.80	0.39	0.41	0.84	0.67	1.18		2.12	2.05
Lu	0.12	0.08	0.10	0.14	0.17	0.14	0.06	0.07	0.12	0.15			0.32	0.29

Major elements in wt.%, trace elements in ppm. FeO* is total iron. Recalculated volatile-free to 100%.

crucial for the development of massive sulphide deposits, but these extreme conditions are not the norm.

The mobility of elements not only depends on the nature and characteristics of the hydrothermal system, but also on the chemistry of the various elements themselves. For example, there are natural groupings of elements that seem to behave in a coherent manner or are not affected by alteration processes. Traditionally, in describing rock chemistry the primary division of elements is based on percentage present, i.e., major (>1 wt.%), minor (0.1—1 percent wt.%) and trace elements (<0.1 percent wt.%). Obviously, element groupings defined in this manner can change, for example, in mafic volcanic rocks of supra-subduction zone settings TiO_2 can range from ~0.1 to > 1.5 percent and K_2O can range from <0.1 to >2 percent. The field strength of elements, i.e., ionic radius/ionic charge, is often used when studying alteration, petrogenesis and tectonic associations of mafic volcanic rocks (Saunders *et al.*, 1980). It, nonetheless, is somewhat inconsistent because Na is not usually defined as a low-field-strength-element (LFSE) even though it is like the LFSEs K, Rb and Cs. Also calcium, an alkaline earth metal like Sr and Ba, is by definition a LFSE, but is never discussed in such a manner. Unfortunately, there is no easy or rigourous way out of this dilemma, except to clearly define those element groups that are to be used during the discussion of element mobility during alteration. These are as follows:

MAJOR ELEMENTS—SiO_2, Al_2O_3, FeO*[2], MgO;
LFSE (low-field-strength-elements)—Ca, Na, K, Mn, Cs, Rb, Ba, Sr, Th, U, Pb;

[2] * Total Fe as FeO

Table 3. Continued

15	16	17	18	19	20	21	22	23	24	25	26	27	28	29	30
1542237	1542046	1542249	1542024	1543354	1542036	1543325	1542116	1543348	1542004	1542266	1542151	1543349	1542267	1543344	1543362
IAT-II	IAT-II	IAT-II	IAT-II	IAT-II	IAT-II	IAT-I	IAT-I	IAT-I	IAT-I	IAT-I	IAT-I	IAT-I	IAT-I	MORB	DACITE
55.4	50.9	51.9	49.9	55.0	52.8	54.1	54.5	51.6	51.8	53.5	56.0	61.4	62.9	50.9	73.8
0.9	0.9	0.9	0.9	1.0	1.2	0.7	0.7	0.8	0.9	1.0	0.9	1.0	1.2	1.5	0.3
15.2	15.9	15.4	15.4	15.2	16.0	13.4	15.7	17.2	15.7	16.3	15.8	13.0	13.4	15.4	13.1
9.1	9.9	10.6	9.9	10.4	12.1	8.3	7.9	10.0	10.3	11.0	10.8	9.3	8.9	10.2	4.6
0.	0.2	0.2	0.2	0.2	0.2	0.2	0.1	0.2	0.2	0.2	0.2	0.2	0.1	0.22	0.1
8.1	8.2	8.5	7.5	6.8	6.4	7.1	6.5	7.7	7.0	6.2	4.7	3.7	3.0	6.6	1.0
7.7	9.9	9.5	12.2	6.6	6.1	12.4	10.7	8.6	10.3	9.3	6.5	7.3	3.6	11.3	0.7
3.3	3.9	2.9	3.9	4.7	4.9	3.7	3.7	3.9	3.7	2.4	4.9	3.9	6.6	3.6	6.1
0.13	0.19	0.15	0.08	0.02	0.36	0.07	0.17	0.06	0.08	0.07	0.09	0.15	0.21	0.15	0.35
0.06	0.04	0.05	0.06	0.10	0.07	0.05	0.04	0.05	0.05	0.07	0.10	0.07	0.09	0.14	0.04
61	60	59	58	54	49	60	59	58	55	50	43	42	38	54	29
2.7	3.4	3.4	3.7	7.4	2.4	1.9	1.8	3.9	2.6	4.2	2.8	1.7	1.1	3.4	1.2
81	166	92	199	23	35	209	94	174	67	61	0	0	22	96	0
37	49	41	57	12	22	76	38	57	30	29	12	0	0	30	0
344	336	347	309	406	464	248	266	284	314	300	439	379	368	311	0
1.0	0.5	0.8	0.8	0.9	0.6	0.5	0.5	0.6	0.8	0.8	1.4	0.9	1.3	3	4.6
32	36	29	37	52	32	32	16	33	37	37	28	54	46	114	162
21	20	21	20	26	26	17	17	23	21	22	21	25	25	36	67
0.28	0.12	0.17	0.12	0.20	0.13	0.13	0.11	0.09	0.22	0.15	0.30	0.20	0.23	0.35	0.74
1.91	1.07	1.34	1.29	1.96	1.29	0.67	0.62	0.94	1.38	1.31	2.60	1.82	2.13	4.22	9.74
5.60	3.80	4.31	4.46	5.81	5.09	2.22	2.26	3.36	4.48	4.68	7.12	6.09	6.75	12.52	24.13
0.88	0.68	0.77	0.79	1.01	0.93	0.44	0.41	0.67	0.74	0.82	1.00	1.10	1.13	2.08	4.22
4.75	4.23	4.80	4.63	5.79	5.70	2.60	2.65	3.97	4.29	5.00	5.28	6.02	6.34	10.82	21.50
1.84	1.66	1.81	1.84	2.18	2.31	1.22	1.25	1.72	1.72	1.96	1.78	2.30	2.24	3.72	7.15
0.76	0.71	0.74	0.87	0.87	0.89	0.48	0.39	0.52	0.73	1.00	0.70	0.69	0.79	1.44	1.55
2.57	2.49	2.41	2.68	3.17	3.43	1.90	1.90	2.52	2.51	2.81	2.54	3.01	3.31	4.78	8.83
0.52	0.51	0.48	0.51	0.63	0.66	0.40	0.42	0.51	0.49	0.57	0.51	0.60	0.64	0.95	1.75
3.82	3.57	3.37	3.65	4.52	4.58	2.85	2.95	3.88	3.52	3.99	3.60	4.18	4.45	6.18	11.95
0.87	0.83	0.78	0.84	1.00	1.05	0.67	0.69	0.88	0.83	0.91	0.87	0.97	1.01	1.38	2.56
2.46	2.33	2.41	2.24	2.91	2.85	1.88	1.94	2.50	2.30	2.58	2.41	2.79	2.84	3.87	7.96
0.35	0.33	0.34	0.32	0.41	0.39	0.28	0.27	0.35	0.33	0.37	0.34	0.40	0.40	0.56	1.19
2.43	2.10	2.34	2.13	2.84	2.65	1.83	1.83	2.30	2.25	2.47	2.32	2.69	2.69	3.53	8.37
0.36	0.30	0.34	0.29	0.45	0.36	0.29	0.27	0.35	0.33	0.35	0.33	0.40	0.37	0.56	1.34

HFSE (high-field-strength-elements)—Ti, P, Y, Zr, Hf, Nb, Ta;
REE (rare-earth-elements)—La, Ce, Pr, Nd, Sm, Eu, Gd, Tb, Dy, Ho, Er, Yb, Lu.

LREE or the light REE—La, Ce, Pr, Nd
MREE or the middle REE—Sm, Eu, Gd, Tb
HREE or the heavy REE—Dy, Ho, Er, Yb, Lu

TE (transition elements)—Cr, Ni, Sc, V

A few points of clarification about these groupings are outlined below:

1) Manganese oxide is usually present at levels of 0.1 to 0.3 percent, i.e., it is on a weight percentage basis a minor element. However, with allocation of Ti and P to the HFSE, a separate minor element grouping seems pointless.

2) Yttrium is left in the HFSE, rather than with the REE (it is not a lathanide). Ti and P are here considered as HFSE as suggested by Saunders et al. (1980).

3) Sodium and Ca are alkali metals and are included in the LFSE.

Methodology

During this study, geochemical sampling was directed primarily toward solving petrogenetic, tectonic, and structural rather than alteration-related problems. Samples displaying anomalous alteration, such as pillow rims, highly fractured rocks, dyke margins, and immediate zones of alteration around massive sulphide deposits, were not collected, except where this complemented the primary aims. Thus, the evaluation of alteration is limited to studying igneous geochemical behaviour on variation diagrams and element ratio plots, to comparisons with presumably equivalent modern rocks, and by constraints derived from experimental and other alteration studies compiled from the literature.

In order to use variation diagrams and element ratio plots to establish igneous trends, it is necessary to plot one element versus an element or element ratio that illustrates the degree of fractionation. In fresh rocks, this is done by using SiO_2 to establish Harker variation plots, by complex ratios (Kuno's Solidification Index or the Differentiation Index), or by ratios based on Fe and Mg, e.g., FeO*/Mgo

Table 4. Composition of Lushs Bight Group dykes (ICP-MS). Each geochemical type is listed in order of decreasing Mg#

Column	1	2	3	4	5	6	7	8	9	10	11	12	13
Sample #	1542206	1543332	1543345	1543361	1543327	1542097	1543346	1543352	1543351	1543331	1543338	1543333	1543359
Group	BON	BON	BON	BON	LOTI	IAT-II	IAT-II	IAT-1	IAT-1	CAB	CAB	CAB	FELSITE(?)
SiO_2	57.0	58.6	60.1	60.7	54.9	52.4	57.0	57.6	62.1	52.7	52.2	53.7	70.5
TiO_2	0.2	0.3	0.2	0.2	0.7	1.0	1.3	0.9	0.8	0.4	0.6	0.6	0.2
Al_2O_3	9.3	15.4	15.4	15.9	15.7	15.1	14.0	15.2	11.8	13.7	12.5	19.0	11.9
FeO*	8.0	8.4	7.7	8.3	8.7	10.7	11.7	12.2	8.6	10.1	10.1	9.0	5.6
MnO	0.2	0.1	0.1	0.1	0.1	0.2	0.2	0.2	0.1	0.2	0.2	0.1	0.1
MgO	11.3	7.3	6.2	3.2	6.5	7.8	4.9	4.5	2.5	10.6	10.3	6.8	0.1
CaO	12.0	6.6	5.3	7.6	8.1	9.0	6.5	4.3	13.4	8.5	10.2	5.1	11.3
Na_2O	2.0	2.9	4.8	3.9	5.0	3.7	4.2	4.4	0.5	3.4	2.5	4.6	0.3
K_2O	0.10	0.41	0.07	0.10	0.29	0.03	0.13	0.54	0.11	0.47	1.19	0.70	0.01
P_2O_5	0.03	0.02	0.03	0.02	0.05	0.06	0.10	0.08	0.07	0.06	0.16	0.30	0.03
Mg#	72	61	59	41	57	56	43	39	34	65	65	57	
LOI	3.9	3.5	2.7	2.2	2.5	2.8	2.2	3.0	1.4	3.6	3.5	4.2	1.2
Cr	1349	46	176	31	226	154			48	496	533		
Ni	337	29	65	11	60	42				106	90		
V	229	278	232	286	292	336	435	448	304	348	351	227	
Nb	1.2	0.6	1.1	1.0	0.8	0.8	1.6	1.4	1.0	1.3	1.4	1.4	2.6
Zr	17	33	43	47	39	44	58	50	57	44	51	62	146
Ti	998	1642	1388	1236	4026	6002	7784	5548	5033	2665	3685	3829	1487
Y	3	5	9	7	18	26	30	19	22	11	14	19	43
Th	0.27	0.41	0.97	0.50	0.22	0.15	0.24	0.53	0.16	1.03	2.20	2.52	0.51
La	1.58	1.75	3.06	2.09	1.41	1.41	2.45	2.53	1.82	5.07	7.57	12.7	4.32
Ce	3.02	3.75	6.25	4.51	3.85	4.83	7.44	6.36	5.31	10.2	15.5	26.0	12.2
Pr	0.32	0.49	0.76	0.57	0.64	0.86	1.29	1.01	0.89	1.33	2.09	3.51	2.07
Nd	1.30	2.01	3.44	2.46	3.66	5.19	6.97	5.22	4.74	5.94	9.08	14.0	10.6
Sm	0.30	0.62	0.93	0.73	1.49	2.04	2.71	1.94	1.78	1.56	2.49	3.34	3.96
Eu	0.16	0.23	0.26	0.32	0.63	0.86	1.01	0.73	0.93	0.54	0.74	1.03	1.40
Gd	0.37	0.71	0.98	0.82	2.15	3.03	3.66	2.27	2.47	1.59	2.32	3.18	5.26
Tb	0.06	0.14	0.18	0.18	0.44	0.61	0.74	0.47	0.49	0.31	0.39	0.55	1.11
Dy	0.48	0.94	1.44	1.23	3.18	4.38	5.12	3.32	3.56	2.05	2.62	3.67	7.90
Ho	0.11	0.22	0.34	0.27	0.72	1.00	1.15	0.75	0.78	0.46	0.56	0.83	1.76
Er	0.34	0.71	1.09	0.85	2.01	2.81	3.38	2.24	2.19	1.42	1.53	2.35	5.44
Tm	0.05	0.11	0.19	0.13	0.29	0.39	0.51	0.36	0.31	0.19	0.23	0.32	0.81
Yb	0.41	0.78	1.35	1.02	1.91	2.74	3.36	2.25	2.15	1.32	1.44	2.37	5.43
Lu	0.07	0.13	0.22	0.18	0.29	0.37	0.50	0.35	0.32	0.22	0.22	0.38	0.80

Major elements in wt.%, trace elements in ppm. FeO* is total iron. Recalculated volatile-free to 100%.

and Mg# (Mg# = atomic Mg/(Mg+Fe). In all of these situations the mobility of the major elements (± LFSE) is a potential, if not major, concern. Furthermore, source heterogeneity can complicate the use of elements, such as Ti, making it difficult to discriminate between coherent behaviour due to alteration and primary petrogenetic effects. For example, formation of secondary muscovite may lead to a fairly coherent K and Rb behaviour that does not reflect their original igneous variation (Figure 9a); whereas the considerable scatter in TiO2 vs K2O (Figure 9b) could be caused by either heterogeneity or alteration. However, the relative coherent behaviour between TiO2 and Zr (Figure 9c) is almost certainly due to primary igneous processes.

A discussion of alteration effects within each of the significant element groupings follows.

Major Elements

Significant mobility in major elements has been documented by a number of workers, (e.g., Pearce, 1975; Coish, 1977); Humphris and Thompson, 1978a). Examination of the types of reactions involved in seawater—basalt interaction (for example, the formation of chlorite and smectite), clearly indicates mobility. In RDHS, Fe and Al are relatively stable and not extensively replaced by Mg (Seyfried, 1987); Si can be either enriched or depleted (Pearce, 1975;

Garcia, 1978). Studies on rim vs core chemical variations in altered pillow lavas (Humphris and Thompson, 1978a) should absolute changes in the ratios of FeO*/MgO and in the Mg# from 0.85 to 1 and 61 to 67, respectively. These changes, on the order of 10 percent, are similar to changes noted in experimental basalt glass—seawater alteration studies (Seyfried et al., 1978) for RDHS. Such variations are thus not necessarily indicative of changes in Fe/Mg in crystalline rocks and demonstrate the reason for avoiding the glassy pillow rims. Alt and Emmermann (1985) have demonstrated that under rock-dominated conditions increasing greenschist facies metamorphism (alteration) of fresh basalt with depth shows no systematic variation in Mg# and that the variation is on the order of 5 percent. Changes in Fe/Mg ratios of 5 to 10 percent during moderate temperature (<400 C), rock-dominated alteration thus presents detailed and reliable fractionation modelling. Alteration is even more intense and pervasive in seawater-dominated alteration, because of the high and prolong acidity.

Low-Field-Strength-Elements (LFSE)

Mobility of these elements is to be expected during alteration in either RDHS or SWDHS, because many of the LFSE are so-called "soluble" elements. However, predicting directions and the magnitude of change can be extremely difficult and dependent on mineralogy (cf. Berger et al., 1988). The formation of spilites (e.g., Cann, 1969; Hughes, 1972) has been a topic of considerable discussion and Hughes (1972) devised a plot to show the variation in Na and K as a result of spilitization. It is generally accepted that Ca, Na and K should not be used to classify altered igneous rocks (Pearce, 1975; Garcia, 1978). Manganese can also be mobilized during alteration, particularly at high temperatures and in SWDHS; however, Mullen (1983) has shown that the behaviour of Mn in some altered rocks, especially relative to the high-field-strength-elements Ti and P, is consistent with that in the primary igneous precursor (see also Bienvenu et al., 1990). Nonetheless, Mullen (1983) noted that in rocks where Ca has been mobile as a result of significant carbonitization Mn behaviour may be suspect. Cesium, Rb, Pb and U are easily mobilized in altered rocks (Palmer and Edmond, 1989; Michard et al., 1983; Bienvenu et al., 1990), and are not useful for identifying primary igneous signatures. The behaviour of Sr and Ba is less well understood and whereas they are certainly mobile, they appear to be less so than Cs, Rb, U, Na and K (Bienvenu et al., 1990). The behaviour of Sr and Ba may be linked to the presence of plagioclase, and how it has been altered. (For example, in the Snooks Arm Group basalts, the behaviour of Sr and Ba was shown to be predictable based on the petrology of the basalts (Jenner and Fryer, 1980)). However, it is generally assumed that they are mobile and not necessarily indicative of the original magma chemistry. Although considered a LFSE, the behaviour of Th appears to be more like that of a HFSE and is generally taken to be immobile during alteration (Wood et al., 1979; Bienvenu et al., 1990). Bienvenu et al. (op. cit.) noted some mobility of Th during alteration of basaltic glass but suggested it could behave differently in crystalline samples.

High-Field-Strength-Elements (HFSE)

The widespread use of HFSE in constructing tectonic discrimination diagrams (Pearce and Cann, 1971, 1973; Winchester and Floyd, 1977; Meschede, 1986) reflects the early recognition that Ti, Y, Zr and Nb are immobile during seawater alteration and metamorphism (Cann, 1970). Geochemical studies of fresh oceanic basalts have shown that the behaviour of Ta and Hf is similar to that of Nb and Zr (e.g., Briqueu et al., 1984), respectively, and their immobility during alteration is predictable (Saunders et al., 1980; Wood et al., 1979; Bienvenu et al., 1990). Winchester and Floyd (1977) suggested limited mobility for P but the mobility was insufficient to significantly alter its discriminant capabilities. Mullen (1983) has also concluded that P can be mobile in cases of severe carbonitization. Finlow-Bates and Stumpfl (1981) concluded that in the intensely altered zones surrounding volcanogenic massive sulphides Nb and Y could be mobile whereas Ti and Zr remained immobile. Their study deliberately made use of extremely altered samples, which were either tuffs or tuffaceous sediments. A study on altered basalts (Williams and Floyd, 1981), using fission track and microprobe studies to trace U and HFSE mobility, found that carbonate complexes can cause element mobility, but it was not clear if elements had actually been lost from the rocks.

Rare-Earth Elements (REE)

Mobility of the REE is one of the most contentious issues in alteration studies of basaltic rocks and there appear to be no simple rules to explain their behaviour (Humphris, 1984). Bienvenu et al. (1990) and Hellman et al. (1979) have suggested that the REE can be mobilized even during low-temperature alteration of basaltic glasses and lavas. Alternatively, others (e.g., Herrmann et al., 1974); Garcia, 1978); Pearce, 1980; and Saunders et al., 1980) have argued that the REE are immobile during low- to moderate-temperature alteration of basalts. The difficulty in understanding REE behaviour reflects our generally poor knowledge of REE complexes at high temperatures and the differences in behaviour of the REE with different dominant fluid species, i.e., chlorine, fluoride and carbonate complexes. Experimental studies by Menzies et al. (1979), Hajash (1984), Sverjensky (1984) and studies of hydrothermal fluids vented on modern oceanic ridges and other environments (Michard and Albarede, 1986) offer some insights.

Table 5. Average compositions for major geochemical groups within the Lushs Bight Group lavas and dykes

Column	1	2	3	4	5	6	7	8
Group	BON	BON	LOTI	LOTI	LOTI-F	LOTI-FH	IAT-II	IAT-II
Type	Lava	Dyke	Lava	Dyke	Dyke	Dyke	Lava	Lava
Mg #	70	66	55	59	44	38	63	48
SiO_2	57.6	57.5	55.0	53.8	54.3	57.3	53.3	53.4
TiO_2	0.1	0.2	0.6	0.4	0.6	0.7	0.8	0.7
Al_2O_3	11.8	13.3	16.2	16.8	17.0	17.1	15.9	14.9
FeO*	8.1	8.1	7.2	8.0	10.1	9.4	9.3	8.0
MnO	0.2	0.1	0.1	0.2	0.2	0.2	0.2	0.2
MgO	11.0	8.9	4.9	7.4	4.9	3.3	8.8	7.5
CaO	8.1	8.8	13.4	10.3	9.3	7.8	7.6	11.4
Na_2O	2.6	2.9	2.5	2.9	2.3	2.7	4.0	3.9
K_2O	0.5	0.1	0.1	0.2	1.2	1.3	0.1	0.1
P_2O_5	0.02	0.02	0.04	0.03	0.10	0.12	0.05	0.04
Cr	715	441	122	85	31		168	235
Ni	153	122	49	45	21		65	79
V	249	263	272	269	314	285	293	256
Nb	1.0	1.3	1.0	0.9	2.3	4.1	0.9	0.5
Zr	21	23	23	18	41	68	33	29
Y	4	6	15	9	19	25	21	16
Th	0.38	0.58	0.25	0.40			0.20	0.15
La	1.28	2.1	1.3	1.4			1.34	1.6
Ce	2.72	4.1	2.6	2.2			4.19	5.7
Pr	0.33	0.53					0.72	0.93
Nd	1.35	2.2	2.7	1.8			4.22	6.7
Sm	0.41	0.6	1.0				1.71	2.7
Eu	0.13	0.2					0.66	1.1
Gd	0.40	0.7	1.6	1.2			2.43	3.9
Tb	0.08	0.13					0.48	0.66
Dy	0.61	0.9	2.4	1.7			3.44	4.7
Ho	0.14	0.22					0.78	1.05
Er	0.50	0.7	1.6	1.3			2.23	3.44
Tm	0.08	0.12					0.32	0.39
Yb	0.66	0.84	1.4	1.1			2.20	3.38
Lu	0.12	0.14					0.32	0.36

Major elements in wt.%, trace elements in ppm. FeO* is total iron. Recalculated volatile-free to 100%.

Both field- and labratory-based studies indicate that Eu can be mobile during alteration processes. This reflects the ability of Eu to exist in divalent or trivalent oxidation states (see Sverjensky, 1984). Interpretation of the origin and/or the magnitude of Eu anomalies in altered volcanic rocks can be contentious (Whitford and Cameron, 1987). If there are strong petrogenetic arguments to support the formation of either a positive or negative Eu anomaly (e.g., Jenner and Fryer, 1980), then a primary igneous origin can be suggested. However, in altered chlorite-rich samples, substantial Eu anomalies may be generated by secondary processes (Whitford *et al.,* 1988).

The potential for internal fractionation within the REE (i.e., LREE versus HREE) and of the REE from the HFSE is also a concern because this may lead to incorrect interpretations of igneous processes and/or to totally obliteration of key petrogenetic and tectonic indicators. While some evidence for elective LREE enrichment exists (Frey *et al.,* 1974; Wood *et al.,* 1976; Hellman *et al.*

Table 5. Continued

9	10	11	12	13	14	15	16	17
IAT-II	IAT-I	IAT-I	IAT-I	IAT	IAT	IAT	MORB	CAB
Dyke	Lava	Lava	Dyke	Lava	Lava	Lava	Dyke	Dyke
54	63	46	51	57	56	56	53	62
52.0	53.4	56.9	54.4	51.7	51.9	52.4	49.9	52.9
1.0	0.7	1.0	0.9	0.8	0.9	0.9	1.6	0.6
15.6	14.9	14.8	15.7	15.6	15.7	15.8	15.4	15.0
10.8	8.0	10.0	10.0	9.4	10.0	10.0	11.1	9.7
0.2	0.2	0.2	0.2	0.2	0.2	0.2	0.2	0.2
7.1	7.5	4.8	6.2	7.1	7.2	7.3	7.1	9.2
9.9	11.4	7.8	8.9	11.8	10.4	9.6	11.3	7.9
3.0	3.9	4.3	3.3	3.3	3.4	3.6	2.7	3.5
0.3	0.1	0.1	0.2	0.1	0.2	0.1	0.5	0.8
0.07	0.04	0.08	0.08	0.07	0.06	0.06	0.15	0.17
108	235	30	122	99	101	109	148	515
37	79	18	33	38	41	39	46	98
354	256	387	325	302	309	320	328	309
1.9	0.5	0.9	1.1	1.5	1.2	0.7	5.5	1.3
45	29	40	43	34	38	35	105	52
27	16	22	24	21	23	21	38	15
0.24	0.15	0.23	0.35	0.12	0.19	0.15		1.9
1.9	1.0	2.2	1.8	1.5	1.6	1.24		8.46
5.3	2.9	6.2	5.0	4.0	4.2	4.15		17.27
1.07	0.44	1.05				0.74		2.31
5.5	3.3	5.4	4.8	4.6	4.9	4.42		9.66
2.2	1.3	2.0	1.8	1.9	1.9	1.77		2.46
1.0	0.48	0.8		0.7	1.1	0.73		0.77
3.5	1.94	2.8	2.6	2.4	3.1	2.56		2.36
0.67	0.40	0.56				0.51		0.42
4.2	2.7	3.7	3.4	3.5	3.6	3.68		2.78
1.08	0.67	0.92				0.84		0.62
2.5	1.88	2.7	2.1	2.0	2.4	2.40		1.77
0.5	0.28	0.37				0.34		0.25
2.6	1.81	2.50	2.5	1.9		2.28		1.71
0.43	0.29	0.37				0.34		0.28

1979; Fryer and Jenner, 1978), studies of hydrothermal fluids, experimental studies and natural rock studies (e.g., Michard and Albarede, 1986; Hajash, 1984; Herrmann *et al.*, 1974; Whitford *et al.*, 1988; Swinden *et al.*, 1990) indicate there is generally little evidence to support significant overall REE mobility or fractionation in RDHS. However, alteration of originally glassy pillow lava rims or the presence of significant amounts of carbonate in the alteration fluids can cause selective REE mobility, especially LREE. Dunning *et al.* (1991) presented evidence for HREE mobility during alteration of mafic volcanic rocks in an Ordovician sequence in central Newfoundland, but the patterns resulting from alteration are clearly different from those of the precursor igneous rocks. However, it is much more difficult to distinguish LREE enrichment during alteration, since the patterns produced can mimic igneous rock patterns. The mere presence of carbonate does not necessarily imply substantial LREE enrichment, for example carbonitized komatiites (Arndt and Jenner, 1986) at Kambalda have LREE depleted

Table 6. Sm—Nd isotopic data for Lushs Bight Group volcanic rocks

SAMPLE NUMBER	GEOCHEMICAL GROUP	$^{143}Nd/^{144}Nd_m$	2 sem	$^{147}Sm/^{144}Nd$	$\epsilon Nd_{(T)}$
1542118	BON	0.512704	20	0.1722	+2.8
1542206	BON	0.512433	10	0.1381	-0.3
1543361	BON	0.512520	17	0.1520	+0.5
1542024	IAT-II	0.513165	20	0.2372	+7.7
1542036	IAT-II	0.513112	13	0.2447	+6.2
1542249	IAT-II	0.513147	18	0.2377	+7.3
1542004	IAT-I	0.513047	32	0.2357	+5.5
1542116	IAT-I	0.513018	05	0.2737	+2.5
1542151	IAT-I	0.513003	20	0.2064	+6.5
1542266	IAT-I	0.513090	11	0.2428	+5.9
1542267	IAT-I	0.513095	10	0.2253	+7.1

Age of 495 Ma used in calculating epsilon values; m = measured, sem = standard error mean
CHUR (today) - $^{143}Nd/^{144}Nd = 0.51264$ & $^{147}Sm/^{144}Nd = 0.1967$
$^{143}Nd/^{144}Nd$ corrected for fractionation to $^{146}Nd/^{144}Nd = 0.7219$
All samples, excluding the boninite dykes 1542206 and 1543361, are from pillow lavas

patterns consistent with their isotopic composition. In summary, there is no *a priori* assumption required that LREE enrichment occurs in all altered volcanic rocks, or even those having significant carbonate content. Conversely care must be taken in sampling and in data evaluation to minimize potential problems and prove internal consistency with other element groups.

Transition Elements (TE)

Scandium, V, Ni and Cr are generally immobile during alteration of komatiites (Arndt and Jenner, 1986), modern ocean-floor basalts (Humphris and Thompson, 1978b; Shervais, 1982), ophiolitic basalts (Pearce, 1975; Coish, 1977; Shervais, 1982) and other basalt types (Winchester and Floyd, 1977). The conditions under which V, Cr and Ni stay immobile extends up to that included in SWDHS (see Seyfried and Mottl, 1982).

GEOCHEMICAL GROUPS

There are three major, and a number of minor, fairly consistent geochemical groups present in both the Lushs Bight Group lavas and dykes and they are illustrated on plots of TiO_2 versus Mg# (Figure 10). However, the stratigraphic and tectonic significance of these groups and their spatial distribution and relationships is still not fully understood. Note that, for example, the sheeted diabase dykes drom different geographic areas have different geochemical constituents. Data from Tables 3 and 4 and the TF-XRF data in Appendix 2 are used in these plots. Table 5 gives the average composition for the major geochemical types.

The most geochemically distinct group of dykes and lavas are the low Ti and high Mg# rocks that are classified as boninites (Figure 10). Primary identification of this group of rocks as boninites was made using an extended REE plot, modified to exclude mobile LFSE (Figure 11). These rocks are also characterized by high SiO_2 (~57 percent) and low Al_2O_3 (see Tables 3, 4 and 5). On the Jensen classification plot (Jensen, 1976) (Figure 12) the boninites plot in the high-Mg tholeiite and basaltic komatiite tectonic environment fields. Their high SiO_2 content, however, does not allow them to be classified on Mullen plots (Mullen, 1983). The boninitic dykes have on average a higher TiO_2 content than the lavas (see Table 5 and Figure 10).

The majority of dykes and lavas in the Lushs Bight Group contain between 0.6 to 1.3 percent TiO_2 and have Mg# between 45 and 65 (Figure 10) and have a broadly dominant tholeiitic nature (Figures 13 and 14). These rocks also show evidence of both Fe and Ti enrichment with increasing degree of fractionation. The majority of the tholeiites are of island-arc origin (Ewart, 1976; Gill, 1981) (Figure 15). This major geochemical group within the Lushs Bight Group is herein referred to as island-arc tholeiite (IAT). The scatter in FeO* and the presence of some calc-alkalic basalts may be due to either alteration or primary processes; although the dataset was previously screened to identify calc-alkaline rocks. A redistribution of

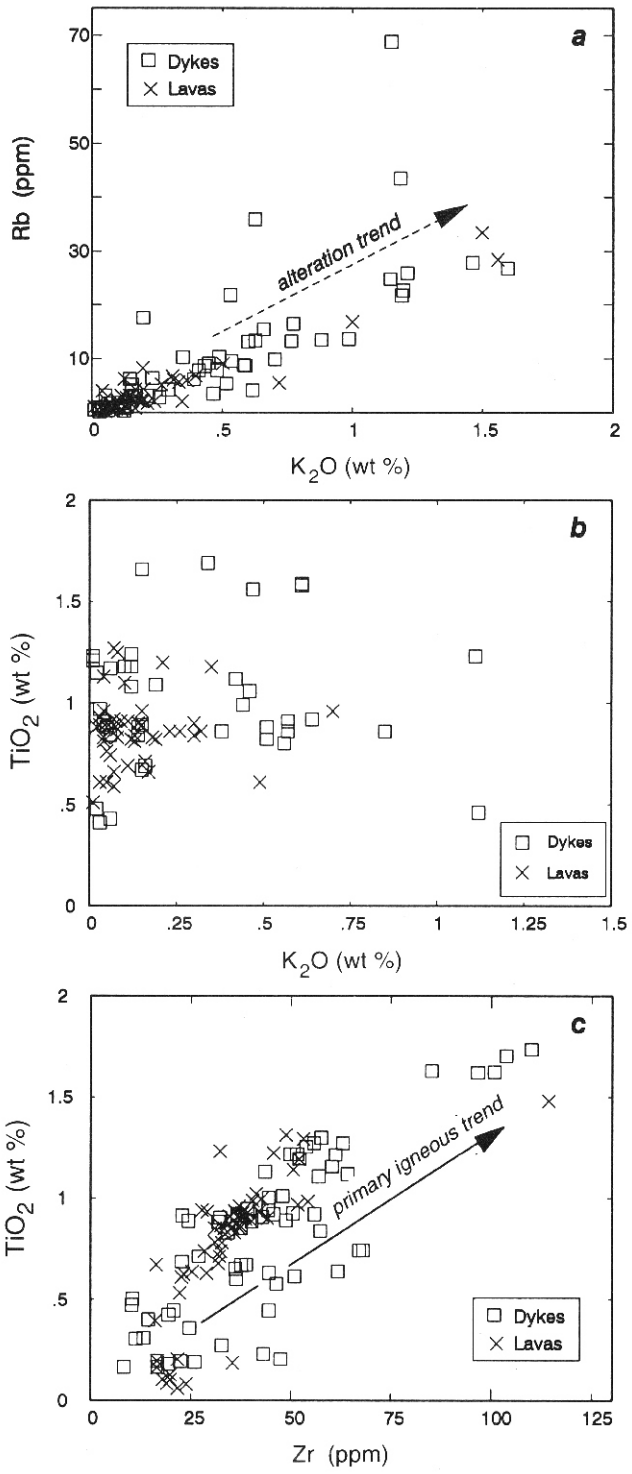

Figure 9. *Comparisons of alteration effects on K_2O, Rb, Zr and TiO_2.*

FeO*, MgO and Al_2O_3 undoubtedly has occurred in these rocks and many of the andesite and basalts actually plot in the continental basalt tectonic field on some ternary diagrams.

Subdivision of the IAT groups into Type I and II is done primarily to highlight the heterogeneity in TiO_2 for a given Mg# (Figure 10) and is not based on any petrogenetic or other geochemical parameters. Figure 13 shows that Type I lavas are slightly displaced toward the Al_2O_3 corner in the AFM plot and they have lower FeO* for a given FeO*/MgO ratio (Figure 14). Differences between Type I and II dykes, although reflected in the TiO_2 content, are generally less evident in the FeO*, MgO and Al_2O_3 content (Figures 13 and 14).

A third geochemical type is characterized by TiO_2 contents intermediate between the IAT and boninites (Figure 10) and is referred to as low titatium tholeiites (LOTI) (cf. Brown and Jenner, 1989). A characteristic feature of the LOTI lavas is their low FeO* relative to FeO*/MgO (see Figure 14). The LOTI lavas plot in either the calc-alkalic or are transitional between the island-arc tholeiitic and calc-alkalic tectonic fields (Figures 13 and 15).

Two dyke samples plot clearly within the LOTI field as defined for the lava field (Figure 10) and an average composition for these is given in Table 5. A third dyke sample plots between the IAT and LOTI fields, but because of its high SiO_2 and low Ti and FeO* relative to rocks with similar Mg#, it is included with the LOTI. An additional ten dyke samples plot outside the LOTI fields and below the IAT field as defined for the lavas. They have been classified as LOTI-FH and LOTI-F (F=fractionated, H=relatively higher Ti) (Figure 10). Samples within these two subdivisions of the LOTI group fall mainly within the tholeiitic field (Figures 13 and 14) with a transgression into the calc-alkalic field (Figure 15).

There are a number of minor and less extensively developed geochemical types within the Lushs Bight Group. A group of lavas and dykes with high TiO_2 and P_2O_5 relative to the boninites, LOTI and IAT, have non-arc signatures and are similar to MORB tholeiites (Figures 10 and 15). Other dykes with high TiO_2, generally > 1.8 percent, have been screened out from the Lushs Bight Group because it could be demonstrated that they were unrelated. Other dykes have a calc-alkalic affinity (CAB) (Figures 10 and 15); all of these dykes intrude the boninitic lavas. Note that the CAB dykes have a Mg # of 57-65. Three dykes do not plot in any of these fields and are included for completion purposes only.

Felsic (dacite—rhyolite) dykes and lavas (Tables 3 and 4) are a minor component of the Lushs Bight Group. The lavas are high in Na_2O and low in K_2O, and have

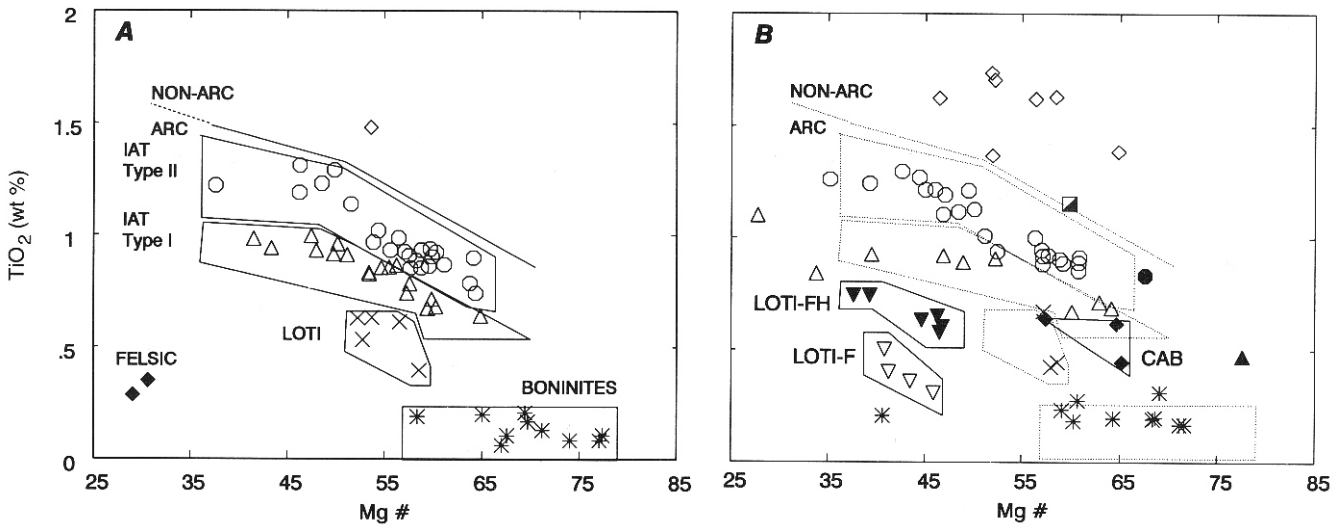

Figure 10. *TiO_2 vs Mg# diagram showing the major geochemical groups in the Lushs Bight Group (A—lavas, B—dykes). Non-arc/arc division line based on complete trace-element evaluations for the Lushs Bight Group and is not intended for use with other rocks. Dotted field boundaries in B indicate groups defined for the lavas; additional groups present only for the dykes are shown by solid lines (e.g., LOTI-FH, LOTI-F, CAB). ◊—Non-ARC; ○—IAT TYPE II; Δ—IAT TYPE I; X—LOTI; ▼—LOTI-FH; ▽—LOTI-F; *—BONINITE; ♦—CALC-ALKALIC BASALTS. Samples 1542099 (**G**), 1542236 (**M**) and 1542289 (▲) are all dykes that do not really conform to the chemical groupings. The felsite or epidosite dyke shown in Table 4 and shown as* **O** *on some plots does not plot on this figure.*

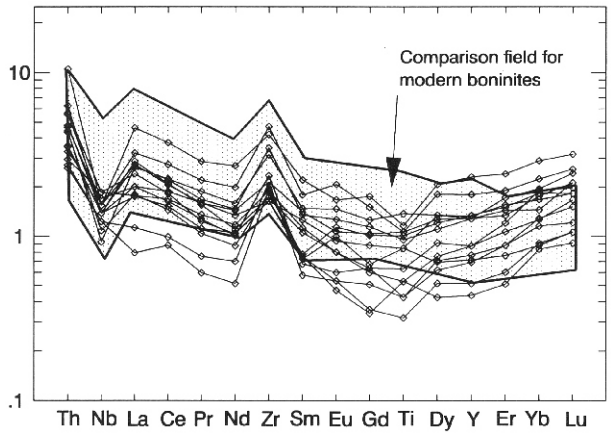

Figure 11. *Primitive mantle normalized plot of selected (immobile) elements for modern boninites and Lushs Bight Group boninites. Data for modern boninites from Jenner (1981, 1982). Normalizing values after Hofmann (1988).*

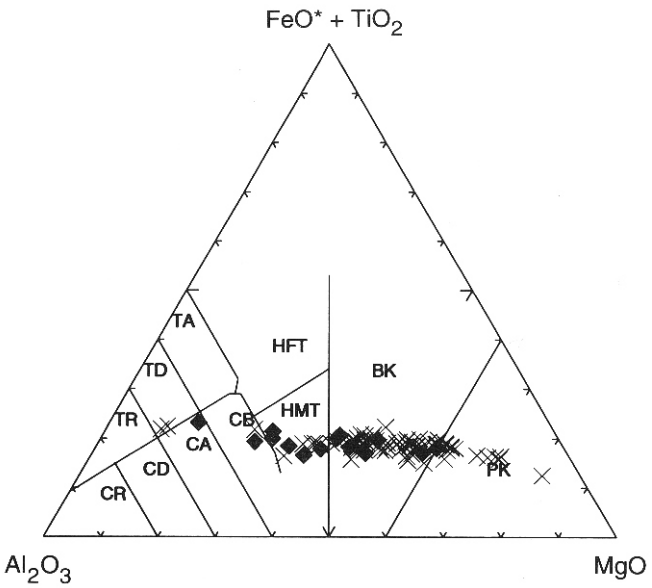

Figure 12. *AFM ternary (cation percent; Jensen, 1976) plot for boninites of the Lushs Bight Group (solid diamonds) and modern boninites (crosses). Data for modern boninites from Jenner (1981, 1982). HFT = high Fe tholeiite; HMT = high Mg tholeiite; BK = basaltic komatiite; PK = peridotitic komatiite; T = tholeiite; C = calc-alkaline. (A = andesite, B = basalt, D = dacite, R = rhyolite).*

similarities to other felsic volcanic rocks in the Notre Dame Bay area (Jenner and Szybinski, 1987; Swinden *et al.*, 1990). The dyke is most likely either a felsite or an epidosite. It is epidotized and has high SiO_2 and CaO and low Na_2O and K_2O contents. It is not plotted on Figure 10 because of its low Mg# and in general, it is not plotted on diagrams using major element ratios. This dyke, from the Little Bay Road area, north of Springdale intrudes Lushs Bight Group dykes, including possibly boninitic dykes.

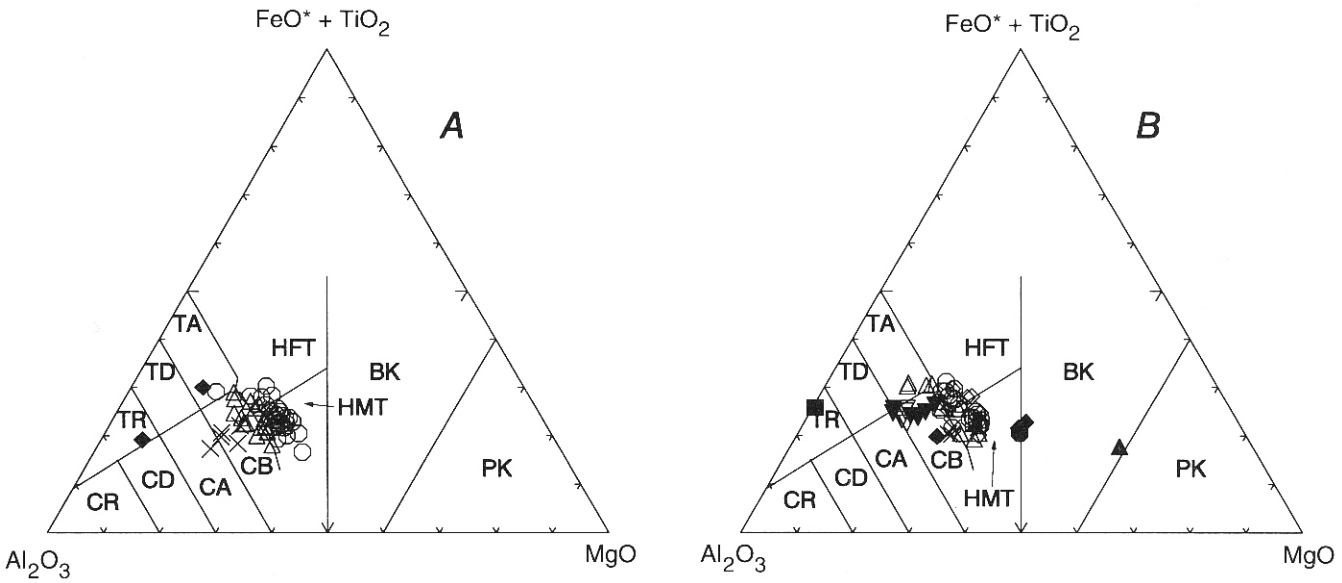

Figure 13. *AFM ternary (cation percent; Jensen, 1976) plot for selected non-boninitic Lushs Bight Group dykes and lavas (A—lavas, B—dykes). Data for modern boninites from Jenner (1981, 1982). HFT = high Fe tholeiite; HMT = high Mg tholeiite; BK = basaltic komatiite; PK = peridotitic komatiite; T = tholeiite; C = calc-alkaline. (A = andesite, B = basalt, D = dacite, R = rhyolite). ◊—Non-ARC; ○—IAT TYPE II; Δ—IAT TYPE I; X—LOTI; ▼—LOTI-FH; ▽—LOTI-F; *—BONINITE; ♦—CALC-ALKALIC BASALTS.*

ROCK CLASSIFICATION

This section attempts to identify the rock types (i.e., basalt, andesite, etc.) that occur in the Lushs Bight Group by using geochemical rock classification diagrams. For this purpose the data is plotted in three major groupings consisting of boninites, non-boninitic dykes and non-boninitic lavas. Both ICP-MS and TF-XRF data are used in the plots.

The boninites, both modern and from the Lushs Bight Group, fall mainly within the andesite and/or andesite—basalt fields (Figures 16 and 17). There is an overlap into the trachyandesite field on the Winchester and Floyd (1977) classifications diagram (Figure 17).

The majority of the non-boninite lavas and dykes straddle the sub-alkaline basalt and andesite—basalt fields (Figures 18 and 19). There is a substantial variation in the Nb/Y ratios; however, this variation is considered to be primarily a source-derived feature. However, the variation in SiO_2 illustrated in Figure 19, i.e., a near vertical trend of increasing SiO_2 at a constant Zr/TiO_2 ratio, is consistent with silica mobility. Silica can increase or decrease with alteration and it is likely then that this trend reflects both possibilities.

INTERPRETATION OF VARIATION DIAGRAMS

The major geochemical groups rather than the major rock types form the basis of discussion in this section because the rock types and/or stratigraphic units do not necessarily form consistent geochemical groups, for example, the different areas of sheeted dyke. Major elements, as defined for this report, are considered unstable during alteration (i.e., mobile) and are not discussed in this section (see discussion on alteration). Boninites and all other geochemical groups are generally plotted on the same diagram.

LFSE

The LFSE are mobile during alteration and it is difficult to compare the concentrations of many of the LFSE with those found in modern rocks. This may sometimes be further complicated by their petrogenesis. Nonetheless, it is instructive to look at the range in Na and K, the most abundant LFSE, utilizing the igneous spectrum plot of Hughes (1972). This diagram of Hughes (*op. cit.*) illustrates the changes in Na and K associated with spilitization. Boninites were not well documented and analyzed until the late 1970s and early 1980s (see Crawford *et al.,* 1989); hence, the "defined" igneous

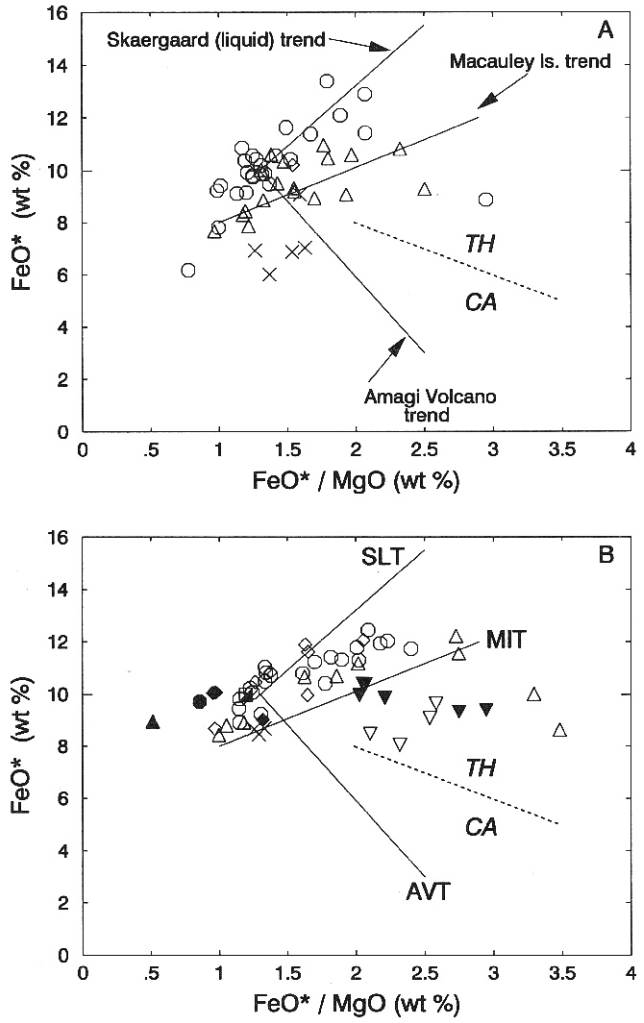

Figure 14. *Modified FeO* vs FeO*/MgO plot (Miyashiro, 1974) for selected non-boninitic Lushs Bight Group dykes and lavas (A—lavas, B—dykes). TH—tholeiitic trend; CA—calk-alkalic trend. ◊—Non-ARC; ○—IAT TYPE II; Δ—IAT TYPE I; X—LOTI; ▼—LOTI-FH; ▽—LOTI-F; *—BONINITE; ♦—CALC-ALKALIC BASALTS.*

spectrum field of Hughes (1972) does not include all of their range (Figure 20). The Lushs Bight Group boninites are depleted in K_2O and generally enriched in $Na_2O + K_2O$ compared to modern boninites. Mean Na_2O in modern boninite rocks is about 1.2 percent, with none greater than 3.6 percent, while in Lushs Bight Group boninites there is a wide, equally distributed range from 0.2 to 5.4 percent. Mean K_2O in modern boninites is 0.45 percent, whereas the content in the Lushs Bight Group ranges from 0.1 to 1.5 percent. The alteration of the Lushs Bight Group boninites draws them towards the field of spilites.

The variation in the K_2O and Na_2O for the non-boninitic Lushs Bight Group rocks is shown in Figure 21. The low-K nature of the volcanism is reflected in this plot, but it is still clear that alteration has displaced the rocks upwards out of the primary igneous spectrum. As was observed by Swinden (1987) in the Wild Bight Group volcanic rocks, there is a greater tendency for the lavas to be displaced toward the spilite field. This is consistent with textural control of alteration, wherein the fine-grained to aphanitic pillow lavas are more altered than the coarser grained dykes.

Transition Elements

The strong positive correlation between Cr and Ni and the Mg# (Figures 22 and 23) is good evidence for their relative immobility during alteration. The Cr and Ni contents show a wide variation that is interpreted to be related to the degree of fractionation, i.e., Mg#. The high Cr and Ni contents of the boninitic lavas and dykes and the high Cr/Ni (>3) ratio are characteristic features of boninites (Jenner, 1981). The Ni content of the IAT group generally falls between 15 to 80 ppm, typical for rocks with this MgO content (cf. Gill, 1981). The Ti vs Cr ratios for the groups (Figure 24) are also typical of orogenic environments; the exception being the non-arc rocks (MORB), which plot within the ocean-floor basalt field. The CAB dykes contain the most surprising Cr and Ni contents, 500 and 100 ppm respectively, (Table 4, also see Table 5), which in conjunction with their relatively high Mg#, suggests they represent atypically primitive calc-alkalic basalt.

Both the boninitic lavas and dykes and the LOTI-F dykes are characterized by Ti/V ratios less than 10 (Figure 25). However, the majority of lavas and dykes in the LOTI, IAT and CAB groups are characterized by Ti/V ratios between 10 to 20, all typical of island-arc volcanic rocks. The MORB-like lava and dykes all have Ti/V >20, typical of non-arc tholeiitic volcanic rocks.

Th and HFSE

General aspects of the variation in Th and HFSE are illustrated in a series of tectonic discrimination diagrams (Figures 26 to 29). Both the boninitic lavas and dykes plot outside any of the tectonic environments on the Ti - Zr and Zr/Y vs Zr diagrams, reflecting both their extremely depleted nature and their high and variable Zr/Y ratios. On the Ti—Zr—Y plot (Figure 28), the boninites fall predominantly in the calc-alkalic basalt field.

Both the IAT and LOTI groups plot within or near the island-arc tholeiite field on all the tectonic discrimination plots in Figures 26 to 28. The non-arc MORB group is distinct from the boninites, LOTI and IAT on the Ti/Zr plot, where it plots distinctly in the ocean-floor basalt

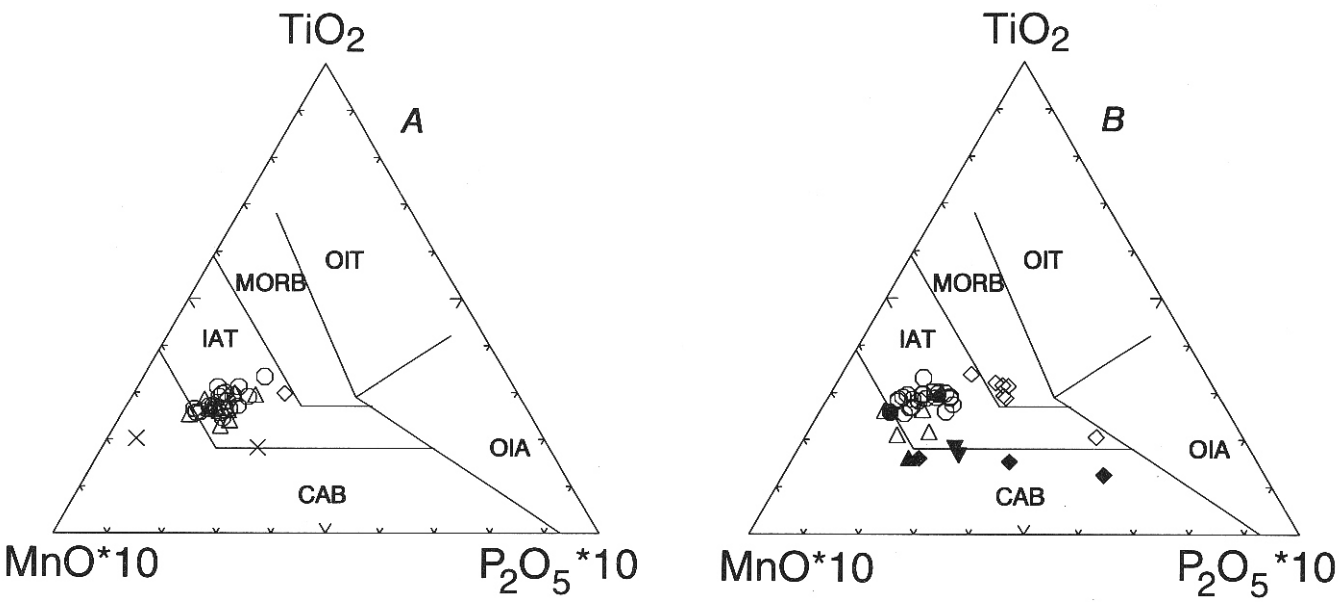

Figure 15. *MnO—TiO_2—P_2O_5 discriminant plot (after Mullen, 1983) for non-boninitic Lushs Bight Group lavas and dykes (A—lavas, B—dykes). OIT—ocean-island tholeiites; OIA—ocean-island basalts; MORB—mid-ocean ridge tholeiites; IAT—island-arc tholeiites; CAB—calc-alkalic basalts. (Note: Plots were screened for samples with silica content between 45 and 54 percent.) ◊—Non-ARC; ○—IAT TYPE II; Δ—IAT TYPE I; X—LOTI; ▼—LOTI-FH; ▽—LOTI-F; *—BONINITE; ♦—CALC-ALKALIC BASALTS.*

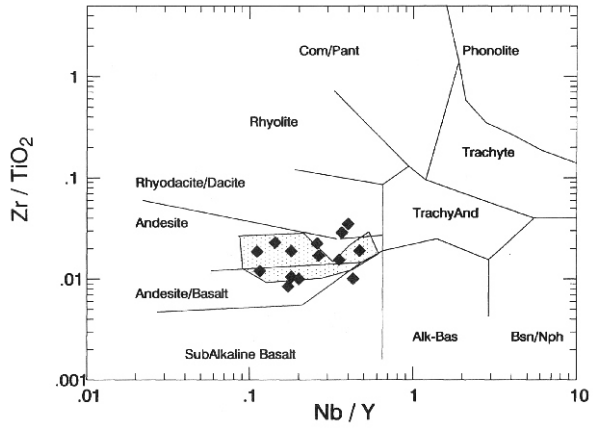

Figure 16. *Zr/TiO_2 vs Nb/Y diagram (Winchester and Floyd, 1977) for Lushs Bight Group boninites. Stippled area is field of modern-day boninites.*

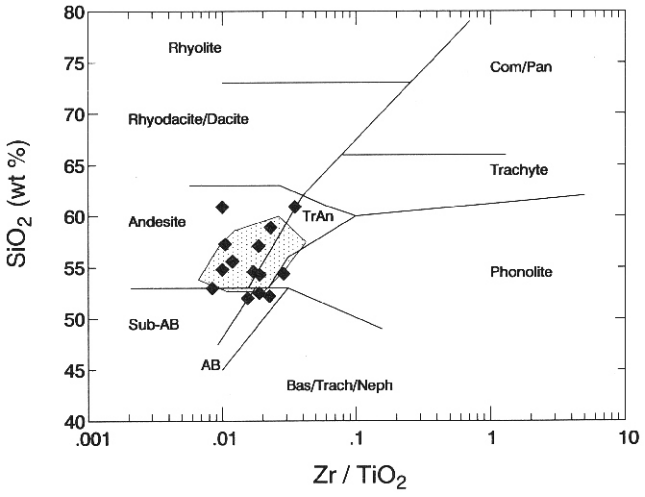

Figure 17. *Zr/TiO_2 vs SiO_2 diagram (Winchester and Floyd, 1977) for Lushs Bight Group boninites. Stippled area is field of modern-day boninites.*

field, it is less distinct on the Zr/Y vs Zr and overlaps considerably on the Ti—Zr—Y plot. Because of their depleted or primitive nature, the CAB dykes are not uniquely defined as calc-alkalic on any of these discrimination plots.

Swinden et al. (1989) devised the discrimination plot Nb/Th vs Y to discriminate between arc and non-arc rocks (Figure 29). The hatched field about the Nb/Th primitive mantle ratio of ~7.4 schematically illustrates a zone of transition between arc and non-arc signatures. A transition in geochemical signature is expected for the following reasons: i) at the low concentrations of Nb and Th found in many oceanic basalts, resolution of the arc-signature (i.e., nagative Nb with respect to Th) will be difficult. Thus only high-quality data should be used in this plot; and ii) since the arc signature reflects mixing of different components, a com-

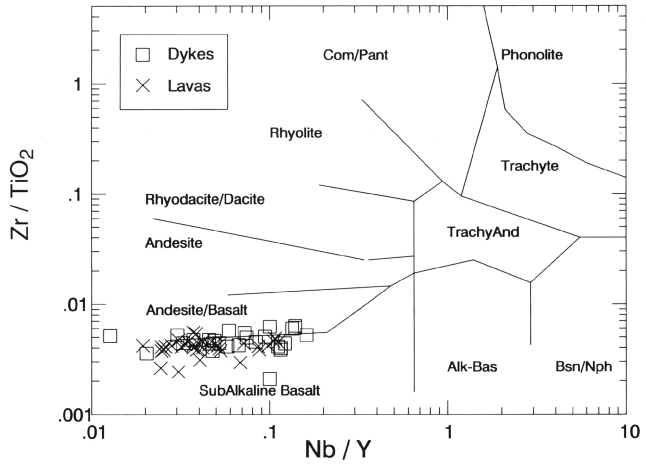

Figure 18. *Zr/TiO_2 vs Nb/Y diagram (Winchester and Floyd, 1977) for selected non-boninitic Lushs Bight Group dykes and lavas.*

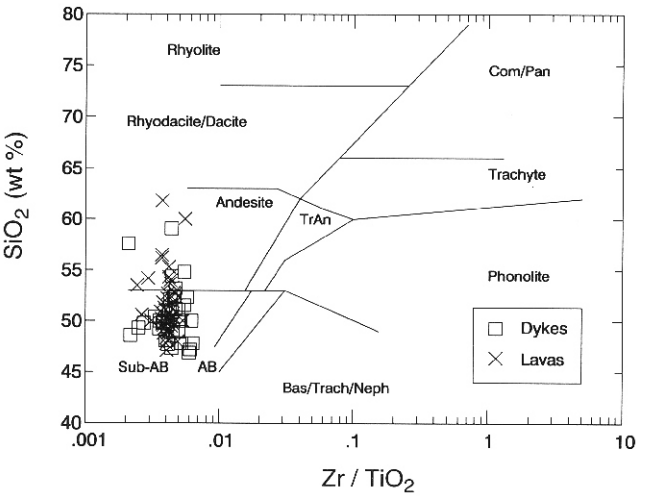

Figure 19. *Zr/TiO_2 vs SiO_2 diagram (Winchester and Floyd, 1977) for selected non-boninitic Lushs Bight Group dykes and lavas.*

plete range of variation can be expected. Not all of the data used in Figure 10 is plotted because there are either no Th analyses or reliable Th analyses available. (Note there are no non-arc (MORB) dykes plotted.) The boninites, LOTI rocks and 2 of the 3 CAB dykes are characterized as refractory arc (RARC) on the diagram, The majority of the IAT group has a clear arc geochemical signature. Note that the three IAT lavas plotting in the non-arc field have Y contents similar to the other IAT, (i.e., significantly lower than that found in the MORB-like rocks) and are also indistinguishable on HFSE discriminant diagrams from the IAT group

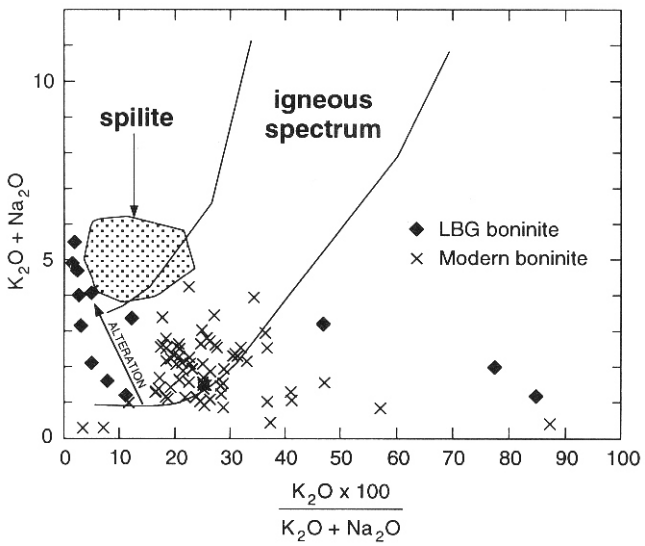

Figure 20. *Modified Hughes (1972) plot illustrating Na and K changes during formation of spilites and alteration of boninites. Lushs Bight Group boninites and modern boninites are solid diamonds and crosses, respectively. (Data source for modern boninites is Jenner, 1981, 1982).*

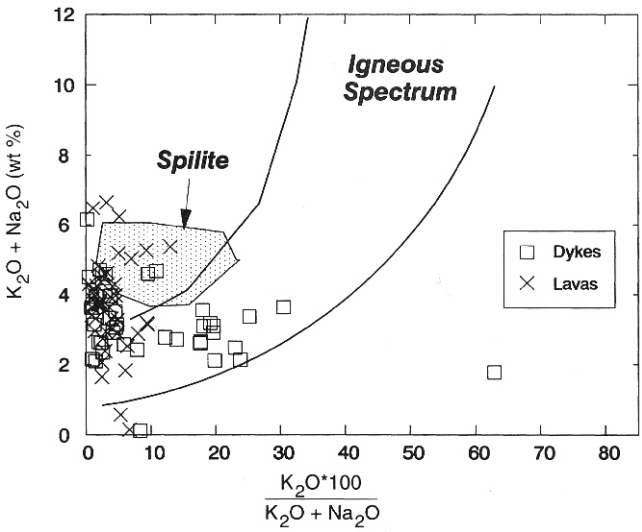

Figure 21. *Modified Hughes (1972) plot illustrating Na and K changes during formation of spilites and alteration of selected Lushs Bight Group dykes and lavas. Note that the lavas are generally more highly altered than the dykes.*

REE

To illustrate the wide variety and complexity of REE patterns in the Lushs Bight Group, the ICP-MS analyses of individual samples are presented as a series of extended

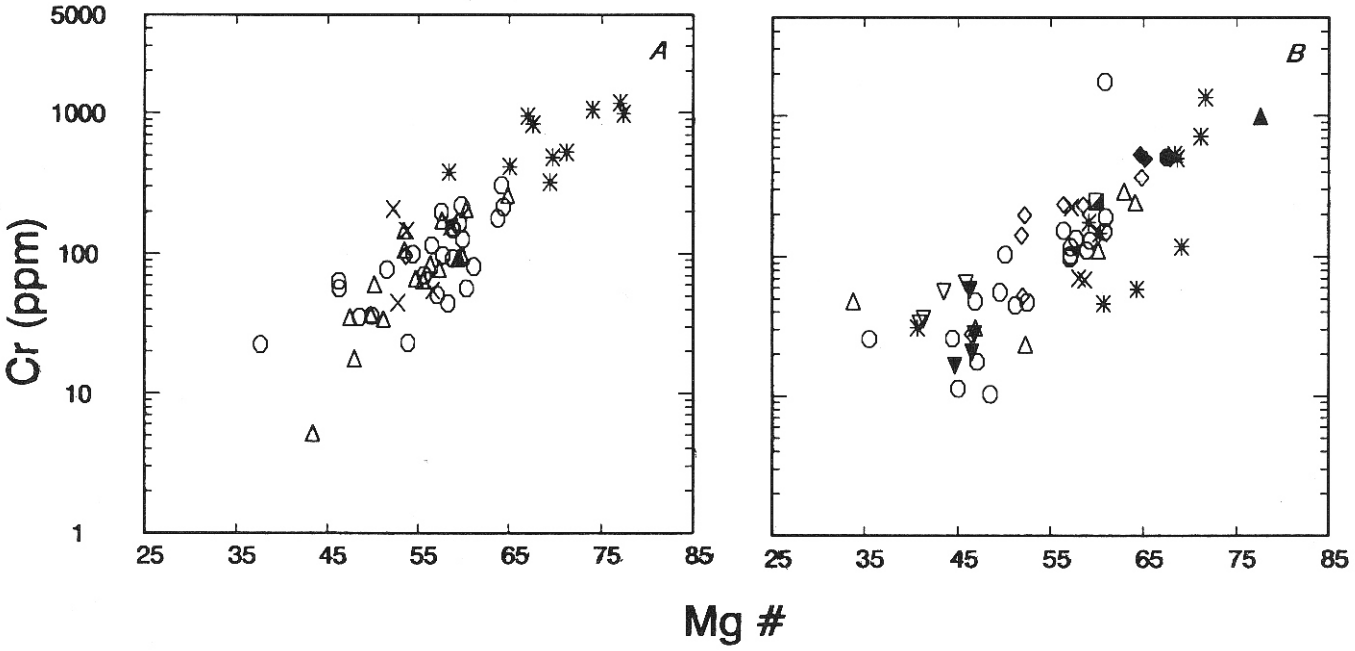

Figure 22. *Log Cr vs Mg#, Lushs Bight Group (A—lavas, B—dykes). ◊—Non-ARC; ○—IAT TYPE II; △—IAT TYPE I; X—LOTI; ▼—LOTI-FH; ▽—LOTI-F; *—BONINITE; ♦—CALC-ALKALIC BASALTS. Samples 1542099 (***G***), 1542236 (***M***) and 1542289 (▲) are all dykes that do not really conform to the chemical groupings. The felsite or epidosite dyke shown in Table 4 and shown as* **O** *on some plots does not plot on this figure.*

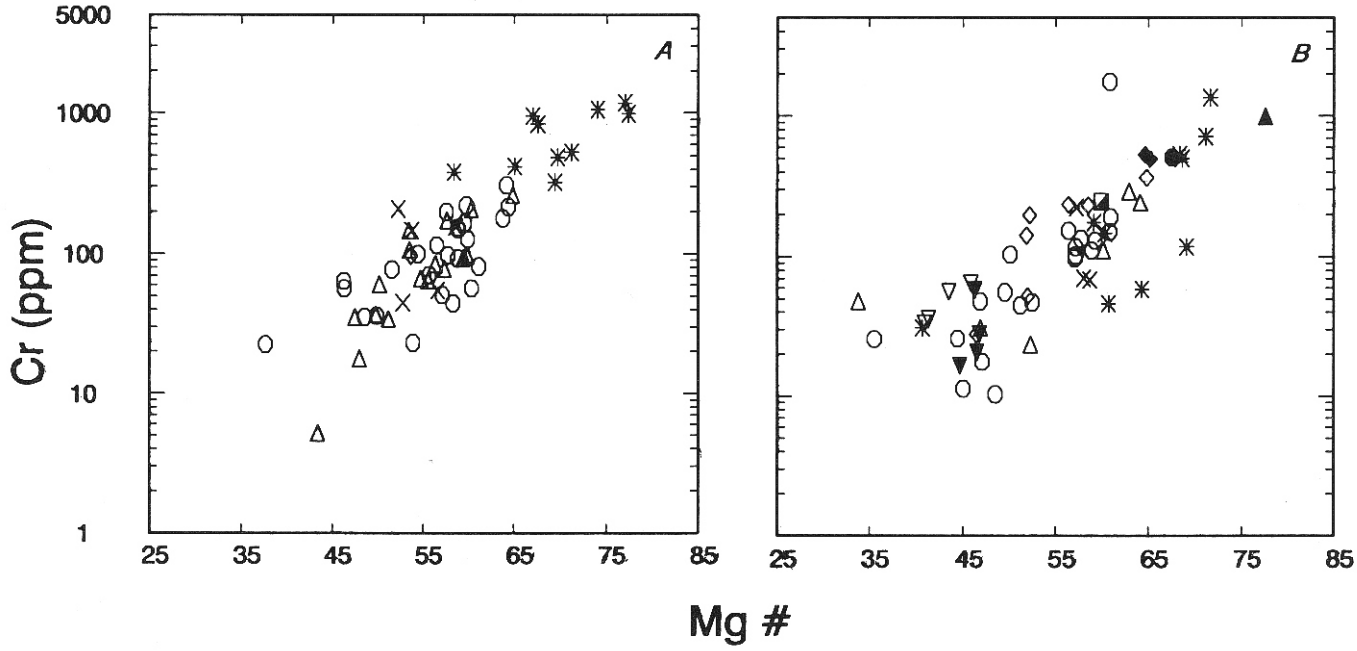

Figure 23. *Log Ni vs Mg#, Lushs Bight Group (A—lavas, B—dykes). ◊—Non-ARC; ○—IAT TYPE II; △—IAT TYPE I; X—LOTI; ▼—LOTI-FH; ▽—LOTI-F; *—BONINITE; ♦—CALC-ALKALIC BASALTS. Samples 1542099 (***G***), 1542236 (***M***) and 1542289 (▲) are all dykes that do not really conform to the chemical groupings. The felsite or epidosite dyke shown in Table 4 and shown as* **O** *on some plots does not plot on this figure.*

REE plots, often with subsets selected on the basis of the Mg# range. Representative fields for the geochemical groups of lavas have been compiled using both the ICP-MS and TF-XRF data. Normalizing values for these plots are primative mantle values from Hofman (1988).

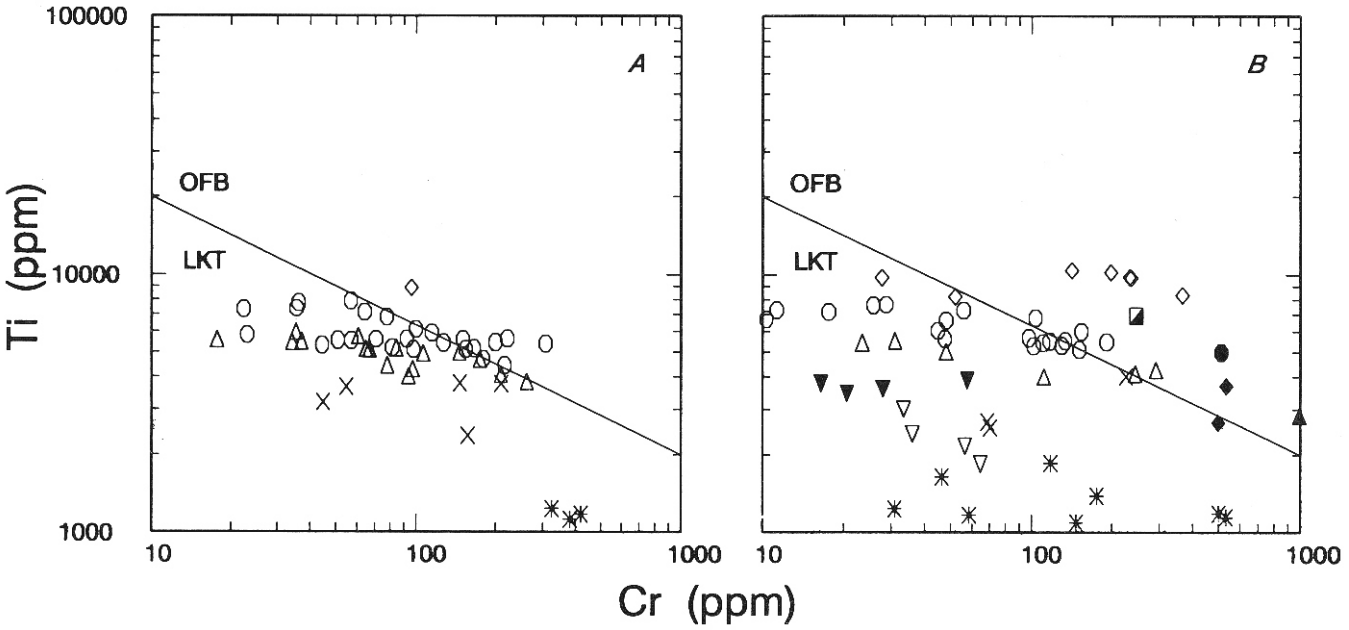

Figure 24. *Ti vs Cr discriminant diagram, Lushs Bight Group (A—lavas, B—dykes). ◊—Non-ARC; ○—IAT TYPE II; △—IAT TYPE I; X—LOTI; ▼—LOTI-FH; ▽—LOTI-F; *—BONINITE; ♦—CALC-ALKALIC BASALTS. LKT—low-potasium tholeiites, OFB—ocean floor basalt. Samples 1542099 (***G***), 1542236 (***M***) and 1542289 (▲) are all dykes that do not really conform to the chemical groupings. The felsite or epidosite dyke shown in Table 4 and shown as* **O** *on some plots does not plot on this figure.*

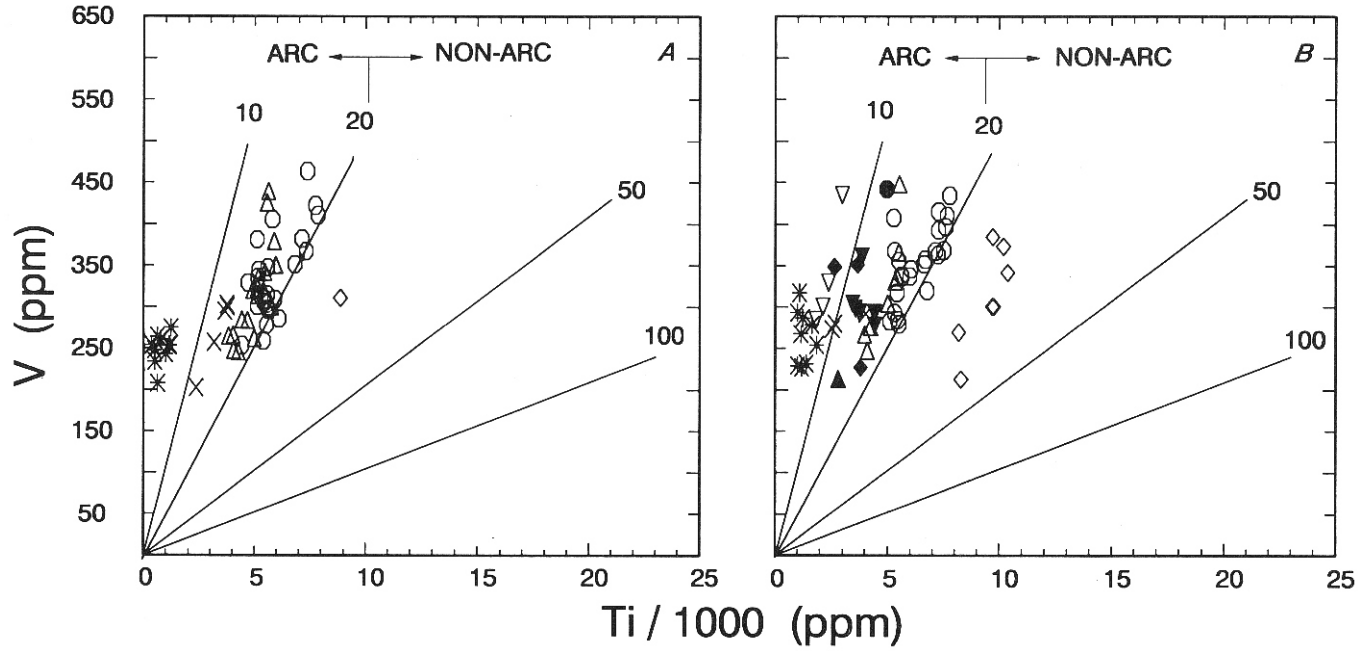

Figure 25. *Ti vs V discriminant diagram (Shervais, 1982), Lushs Bight Group (A—lavas, B—dykes). ◊—Non-ARC; ○—IAT TYPE II; △—IAT TYPE I; X—LOTI; ▼—LOTI-FH; ▽—LOTI-F; *—BONINITE; ♦—CALC-ALKALIC BASALTS. Labelled lines represent constant Ti/V ratios. Samples 1542099 (***G***), 1542236 (***M***) and 1542289 (▲) are all dykes that do not really conform to the chemical groupings. The felsite or epidosite dyke shown in Table 4 and shown as* **O** *on some plots does not plot on this figure.*

Lavas

The extended REE pattern for the boninitic rocks is characterized by Th enrichment relative to La, positive Zr relative to Sm and Nd, and a concave pattern with MREE depletion relative to LREE and HREE (Figure 30). Generally, there is a negative Nb anomaly relative to Th and La. Samples 1543336 and 1543337 do not show this

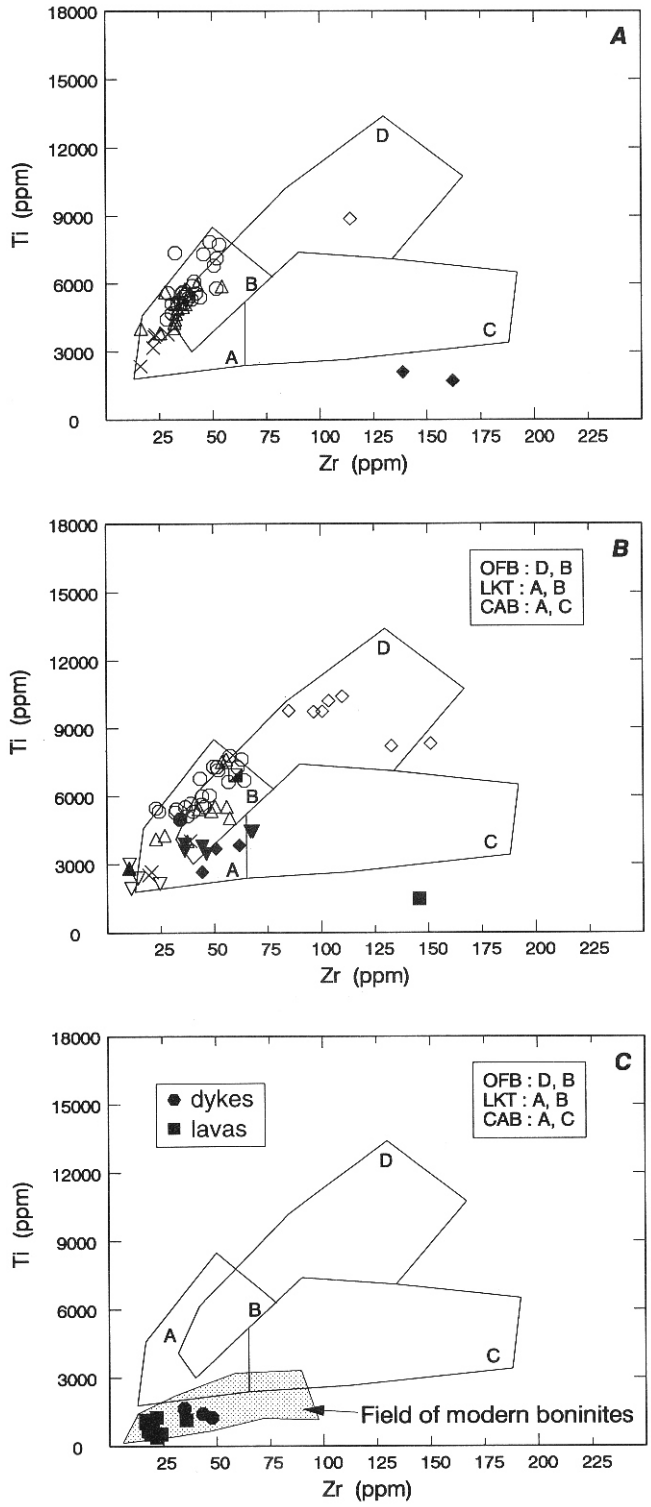

Figure 26. *Ti vs Zr discriminant diagram (Pearce and Cann, 1973), Lushs Bight Group (A—lavas, B—dykes, C—boninites). ◊—Non-ARC; ○—IAT TYPE II; Δ—IAT TYPE I; X—LOTI; ▼—LOTI-FH; ▽—LOTI-F; *—BONINITE; ♦—CALC-ALKALIC BASALTS. Samples 1542099 (***G***), 1542236 (***M***) and 1542289 (▲) are all dykes that do not really conform to the chemical groupings.*

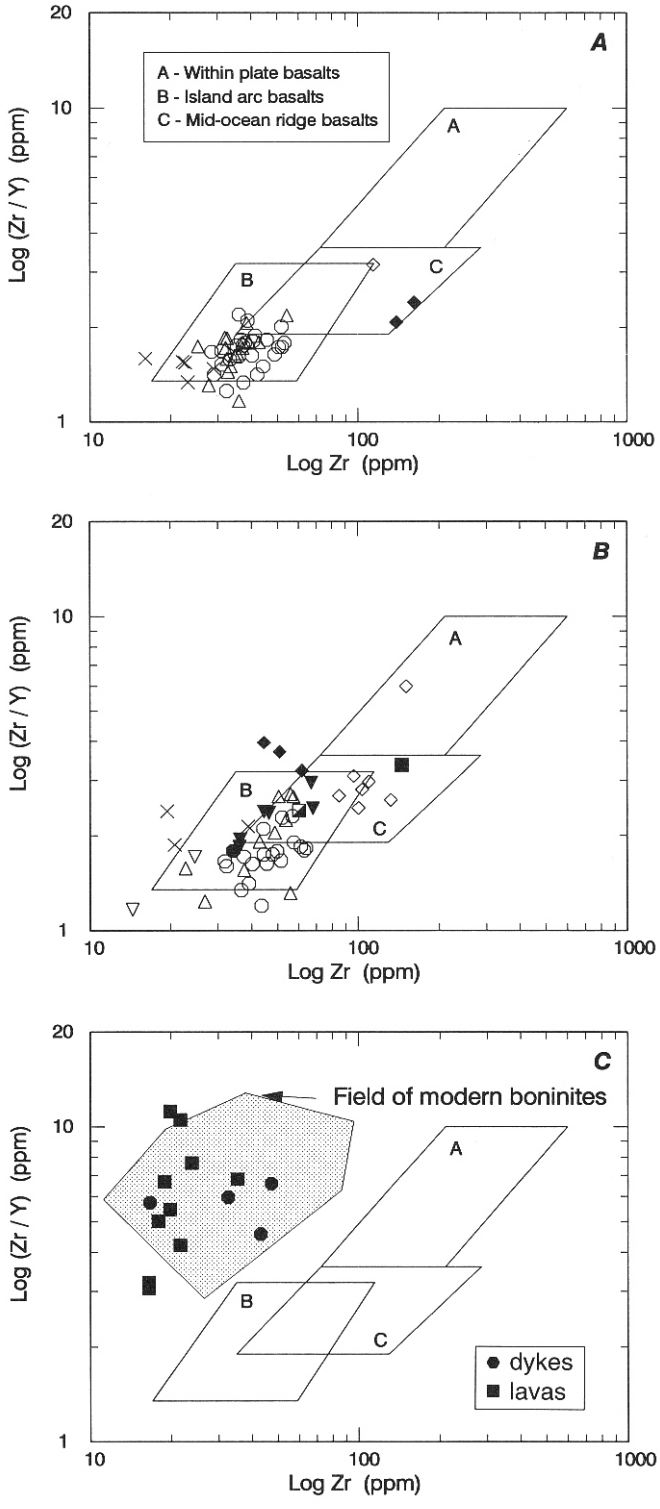

Figure 27. *Zr/Y vs Zr discriminant diagram (Pearce and Norry, 1974), Lushs Bight Group (A—lavas, B—dykes, C—boninites). ◊—Non-ARC; ○—IAT TYPE II; Δ—IAT TYPE I; X—LOTI; ▼—LOTI-FH; ▽—LOTI-F; *—BONINITE; ♦—CALC-ALKALIC BASALTS. Samples 1542099 (***G***), 1542236 (***M***) and 1542289 (▲) are all dykes that do not really conform to the chemical groupings.*

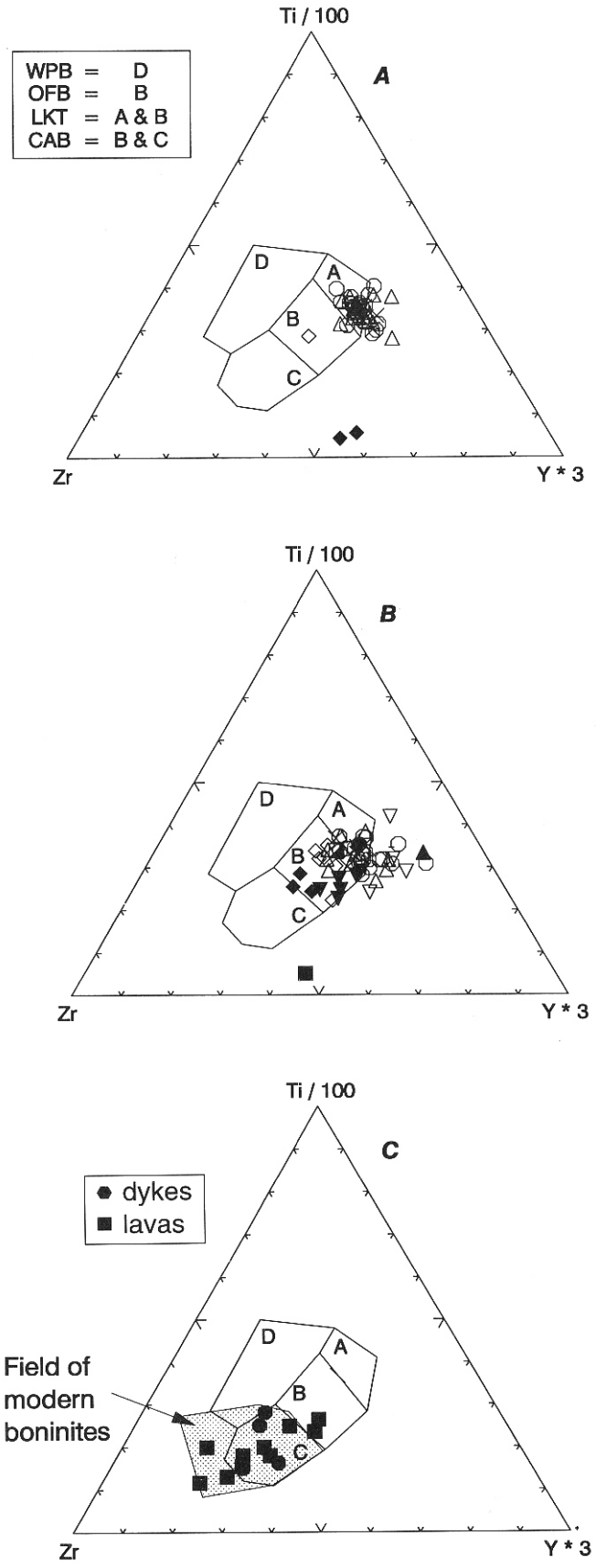

anomaly and are overall depleted in REE. Many samples show crosscutting patterns and heterogenities in abundances relative to Mg#. Some samples having parallel patterns could be related by low-pressure fractionation of the appropriate liquidus phases, presumably olivine ± orthopyroxene (Jenner, 1981, 1982) e.g., samples 1543329, 1543365 and 1543334. Samples 1543335 and 1552118 have Mg#s of about 67, and their pattern is consistent in shape and abundance with that present for the more primitive boninites. Sample 1543347, the least primitive boninite (Mg#58), has a similar pattern and abundances to that observed in most of the other boninites.

There is considerable variation in REE abundances and patterns in the IAT group (Figure 31). The following features are noteworthy: i) Type I are generally the most depleted, particularly in HREE, ii) all of the samples have negative Nb with respect to Th, but Th is not necessarily enriched relative to La, iii) Ti and Y behaviour is consistent with that of the REE, while Zr can be depleted relative to Nd—Sm, iv) all samples exhibit LREE depletion, and the patterns are often crosscutting either in LREE or HREE, and v) overall there is a slight increase in REE and HFSE with fractionation. This is consistent with a low pressure fractional crystallization of olivine ± clinopyroxene ± plagioclase as likely phases.

The variability in abundance of REE and in pattern shape within the IAT is well illustrated in Figure 32. The subdivision into Type I and II based on Mg# and Ti (see Figure 10) oversimplifies the chemical diversity of this group, particularly with regards to Th, Nb and the LREE. Both the trace elements and REE for the IAT group suggest that their extended REE pattern for any given set of Mg#s is a combination of source-derived characteristics and low pressure fractional crystallization.

The LOTI group is enriched in HREE relative to the boninites (see Figure 32), is overall LREE depleted and lacks evidence for positive Zr relative to Nd and Sm (Figure 33), possibly linking their petrogenesis more to the IAT lavas. Compared to the IAT lavas in the Mg# 50-59 range (see Figure 32), there is some similarity in Th through Nd, but they are depleted with respect to Zr through Lu. All the patterns have negative Nb with respect to Th.

Figure 28. *Ti—Zr—Y discriminant diagram (Pearce and Cann, 1973), Lushs Bight Group (A—lavas, B—dykes, C—boninites). ◊—Non-ARC; ○—IAT TYPE II; △—IAT TYPE I; X—LOTI; ▼—LOTI-FH; ▽—LOTI-F; *—BONINITE; ♦—CALC-ALKALIC BASALTS. Samples 1542099 (***G***), 1542236 (***M***) and 1542289 (▲) are all dykes that do not really conform to the chemical groupings.*

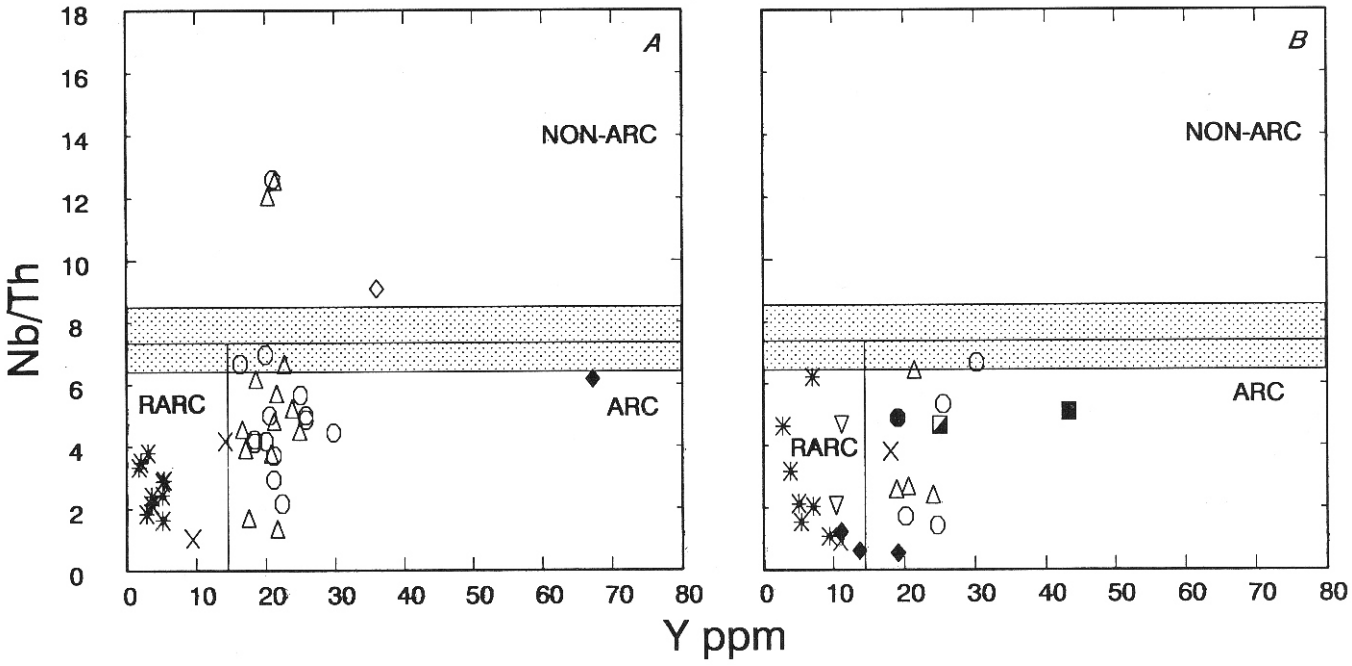

Figure 29. *Nb/Th vs Y discriminant diagram (Swinden et al., 1989), Lushs Bight Group (A—lavas, B—dykes). ◊—Non-ARC; ○—IAT TYPE II; △—IAT TYPE I; X—LOTI; ▼—LOTI-FH; ▽—LOTI-F; *—BONINITE; ♦—CALC-ALKALIC BASALTS. Samples 1542099 (***G***), 1542236 (***M***) and 1542289 (▲) are all dykes that do not really conform to the chemical groupings. Samples in the non-arc field are 1543344, 1542013, 1542027 and 1542034.*

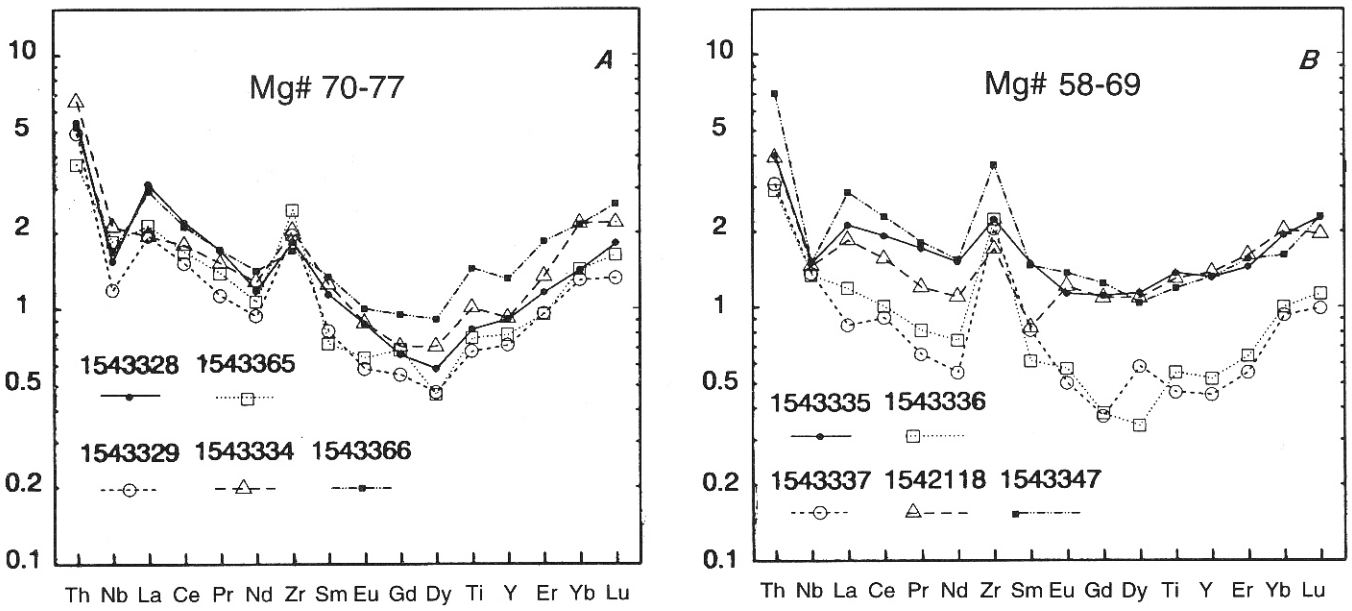

Figure 30. *Primitive mantle normalized extended REE patterns for boninitic rocks of the Lushs Bight Group (A—Mg# 70-77; B—Mg# 58-69).*

The lava classified as a MORB (sample 1543344) on most of the discriminant diagrams is characterized by the lack of a well defined negative Nb anomaly and overall low HFSE and REE abundances (Figure 34). It is part of a black, hematitic (generally more chlorite -rich than epidote-rich), pillow basalt phase that in places marks the top of the Lushs Bight Group near the contact with the Western Arm Group in the Clam Pond area. The other

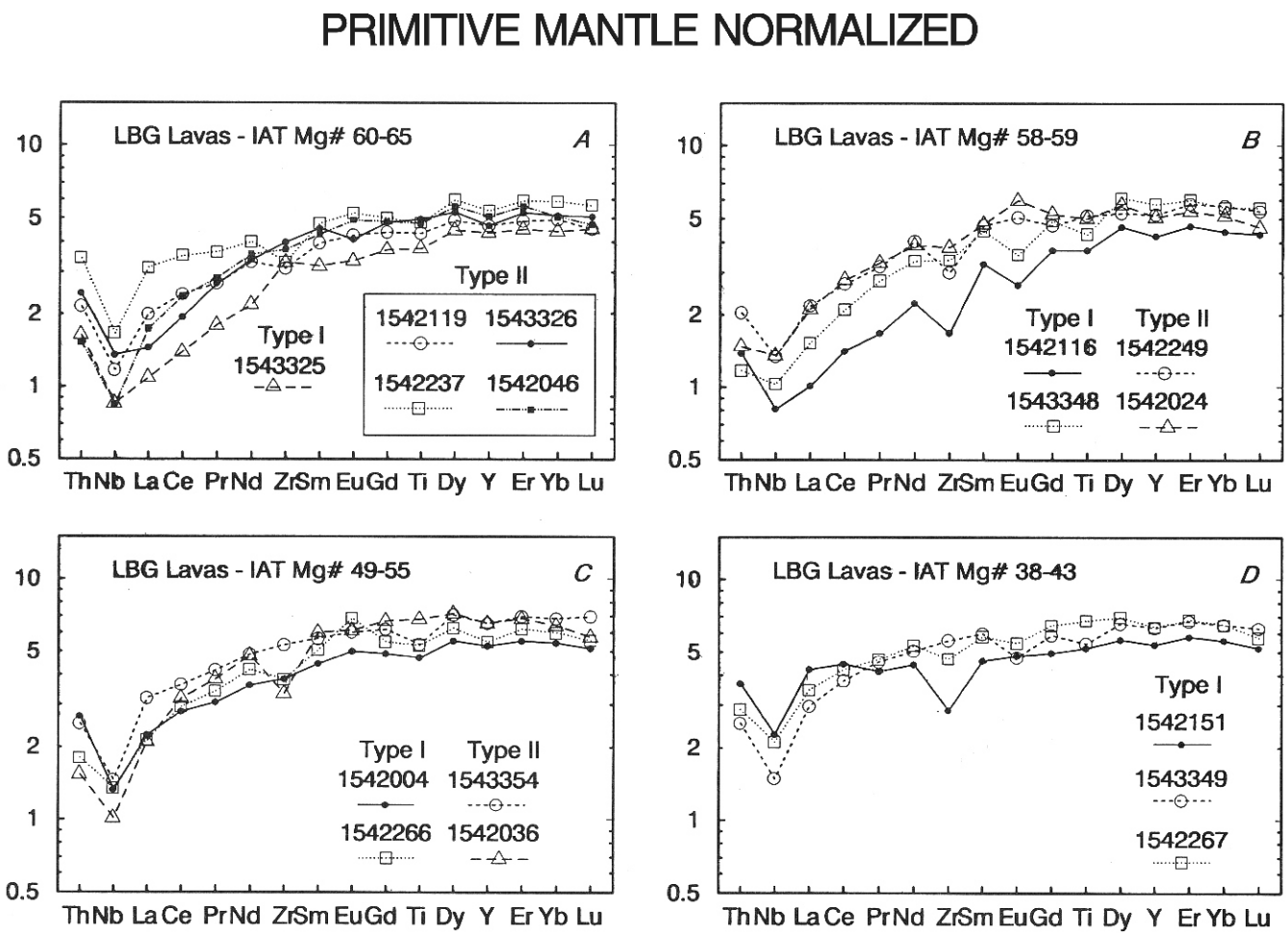

Figure 31. *Primitive mantle normalized extended REE patterns for IAT lavas, Lushs Bight Group.*

three lava samples were distinguished as non-arc only on the Nb/Th vs Y diagram. They all come from the Southern Arm area and are all intruded by IAT group dykes. They are LREE-depleted and with the exception of a negative Nb anomaly, have concentrations of REE and HFSE similar to most of the island-arc tholeiites, i.e., much lower than MORB.

Dykes

Extended REE patterns for Lushs Bight Group dykes are given in Figure 35. The boninitic dykes are characterized by Th enrichment relative to Nb and La, by negative Nb anomalies, by concave REE patterns and enrichment in Zr relative to Nd and Sm. Sample 1542206 is the most primitive sample (see Table 4) and is characterized by lower abundance of all elements except Nb. Samples 1543332 and 1543345 have similar Mg#, but the latter sample is enriched in all elements, excluding Ti, by a factor of 1.3 to ~2. The dykes are enriched in LREE and Th relative to the lavas.

The dykes of the IAT and LOTI groups have a large range in Mg#, thus making detailed comparisons difficult. In general, both these groups are LREE depleted, and there is considerable variation in Th, Nb, La. All have negative Nb, but not all have Th enrichment. The LOTI sample and IAT-II sample 1542097 have similar Mg#s, and are quite similar in La and Nb. They differ most in elements less compatible than Nd (i.e., Nd—Lu) and the LOTI sample has a Th enrichment compared to sample 1542097. The IAT-II samples have essentially parallel patterns, with the least primitive sample having the higher element abundances. This is consistent with a low-pressure fractional crystallization petrogenesis. Patterns in the IAT-I group samples crosscut each other, the most notable example being shown by the LREE enrichment in sample 1543352. The IAT-I samples are depleted in HREE, Ti and Y relative to the more primitive IAT-II group (see Mg#s in Table 4). IAT-I sample 1543352, however, is enriched in Th, Nb, LREE and Zr relative to the most primitive IAT-II sample (1542097).

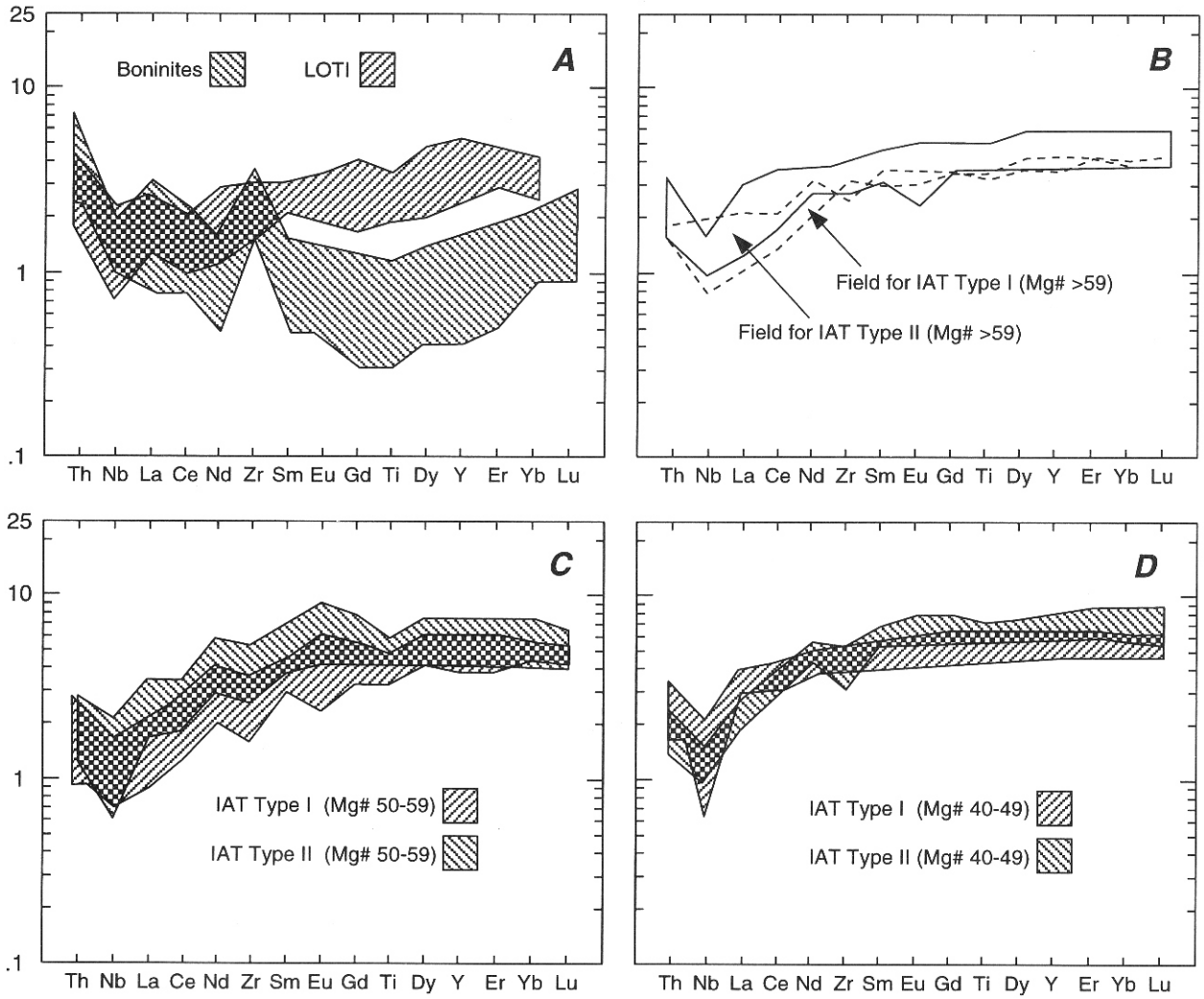

Figure 32. *REE-pattern fields for the different Lushs Bight Group lava groups (combined ICP-MS and TF-XRF data).*

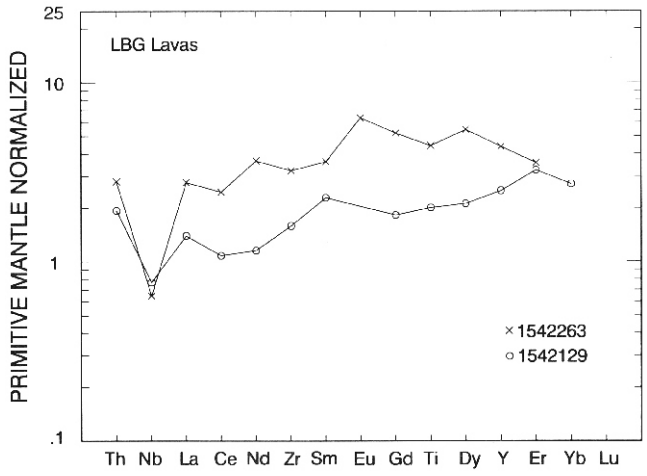

Figure 33. *Primitive mantle normalized extended REE patterns for LOTI lavas, Lushs Bight Group.*

The calc-alkalic dykes, all intrusive into the boninitic lavas, are characterized by Th enrichment relative to La,by well developed negative Nb anomalies, and by LREE enrichment. Samples 1543338 and 1543333 have slight negative Zr anomalies and the latter also has a negative Ti anomaly. They have similar high Mg# and Cr and Ni contents, but show considerable variation in Th, LREE, Ti and Zr abundances. Considering their overall chemical similarity, these samples could represent either magmas derived from a heterogeneous source, or by different degrees of partial melting of the source. In the latter case, sample 1543338 would represent a smaller degree of partial melting and sample 1543333 could possibly be derived from sample 1543338 by low-pressure fractional crystallization.

There is no REE data available for the non-arc (MORB) dykes.

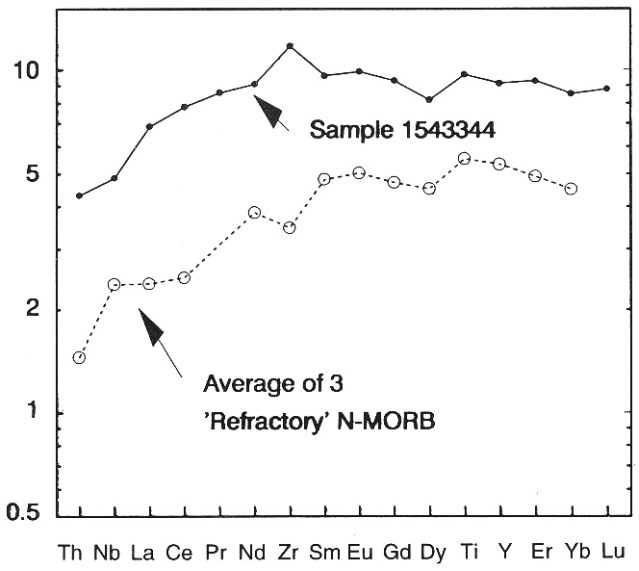

Figure 34. *Primitive mantle normalized extended REE pattern for Lushs Bight Group non-arc lavas. The three samples averaged are 1542013, 1542027 and 1542034.*

Felsic Rocks

Two samples of Lushs Bight Group felsic rocks were analysed for REE and Th (Figure 36). Sample 1543362 is a felsic volcanic characterized by i) abundances of REE 15 to 20 times primitive mantle, ii) LREE depletion, iii) strong negative Eu anomaly, and iv) a negative Nb anomaly. The major- and trace-element characteristics of this sample indicate that it could be derived by low-pressure fractional crystallization.

Sample 1543359 is from an altered, epidotized dyke, which is interpreted to cut boninitic dykes near Springdale. It is characterized by low REE concentrations in the order of 5 to 12 times primitive mantle, by LREE depletion, by a negative Nb anomaly and by a positive Zr anomaly. The petrogenesis of this rock is unclear, but it could be an altered andesite—dacite dyke with affinities to LOTI or IAT-I.

Sm—Nd Isotopes

To augment the trace-element data and provide a representative suite for a regional isotopic study, Sm—Nd isotopic compositions were determined on 11 samples from the Lushs Bight Group (Table 6).

The three boninite samples range in initial isotopic composition (Nd(T)) from +2.8 to -0.3. This range in isotopic composition is positively correlated with $^{147}Sm/^{144}Nd$, and overlaps with other Newfoundland boninites (Figure 37). It is consistent with the addition of an enriched component to a depleted mantle source.

The eight non-boninitic Lushs Bight Group samples are all from the IAT group and have Nd(T) values ranging from +7.7 to +2.5, with the lowest value occurring in sample 1542116. The low Nd(T) and high 147Sm/144Nd in 1542116 places it in the refractory arc volcanic field (RARC). The remaining seven samples have two distinct clusterings made up of a group of four samples (1542024, 1542249, 1542267, 1542151) with Nd(T) ranging from +6.5 to +7.7 and a second group of three samples (1542004, 1542036, 1542266) with values from +5.5 to +6.2. Both of these clusters contain samples from both Type I and II of the IAT group. Six out of the above seven samples plot within island-arc tholeiite fields defined by all Newfoundland Ordovician volcanic rocks and are characterized by Nb/Th ratios of ~5. One sample (1542024) has a Nb/Th ratio of 6.7 and plots in the arc-transitional-MORB field (ATM).

Summary

Hydrothermal alteration and metamorphism of oceanic basalts can lead to substantial changes in their chemical composition. As an element group the LFSE are more susceptible to alteration, than the HFSE, REE, TE and some major elements. A subset of the LFSE (K, Na, Ca, Cs, Rb, U and Pb) should be considered mobile and not used in classifying the primary igneous characteristics of altered volcanic rocks, or in defining the tectonic environment of formation. However, Mn and Th, particularly Th, are immobile or often only slightly mobile, and in conjunction with HFSE are useful in defining rock types and environments of formation. The TiO_2—P_2O_5—MnO plot devised by Mullen (1983) appears to work well.

However, there is less evidence to support significant mobility of the HFSE, TE, and REE. It is important to reiterate that the use of the term "significant mobility" means that while elements may have undergone some degree of mobilization, they have done so in a coherent manner which does not preclude recognition of their original source-derived characteristics. The mobility of TE, REE and HFSE and Mn and Th is normally most significant in the presumably fine-grained and depleted boninites. In general, when elements in these element-groupings are mobile, the patterns on extended REE plots clearly indicate this (Dunning et al., 1991). There may, however, be more subtle variations that are not detected or obvious, for example in the LREE. However, the REE, Th and HFSE are consistent with that observed in equivalent modern settings and with Sm—Nd isotopic values (Swinden *et al.*, 1990; Jenner *et al.*, 1991).

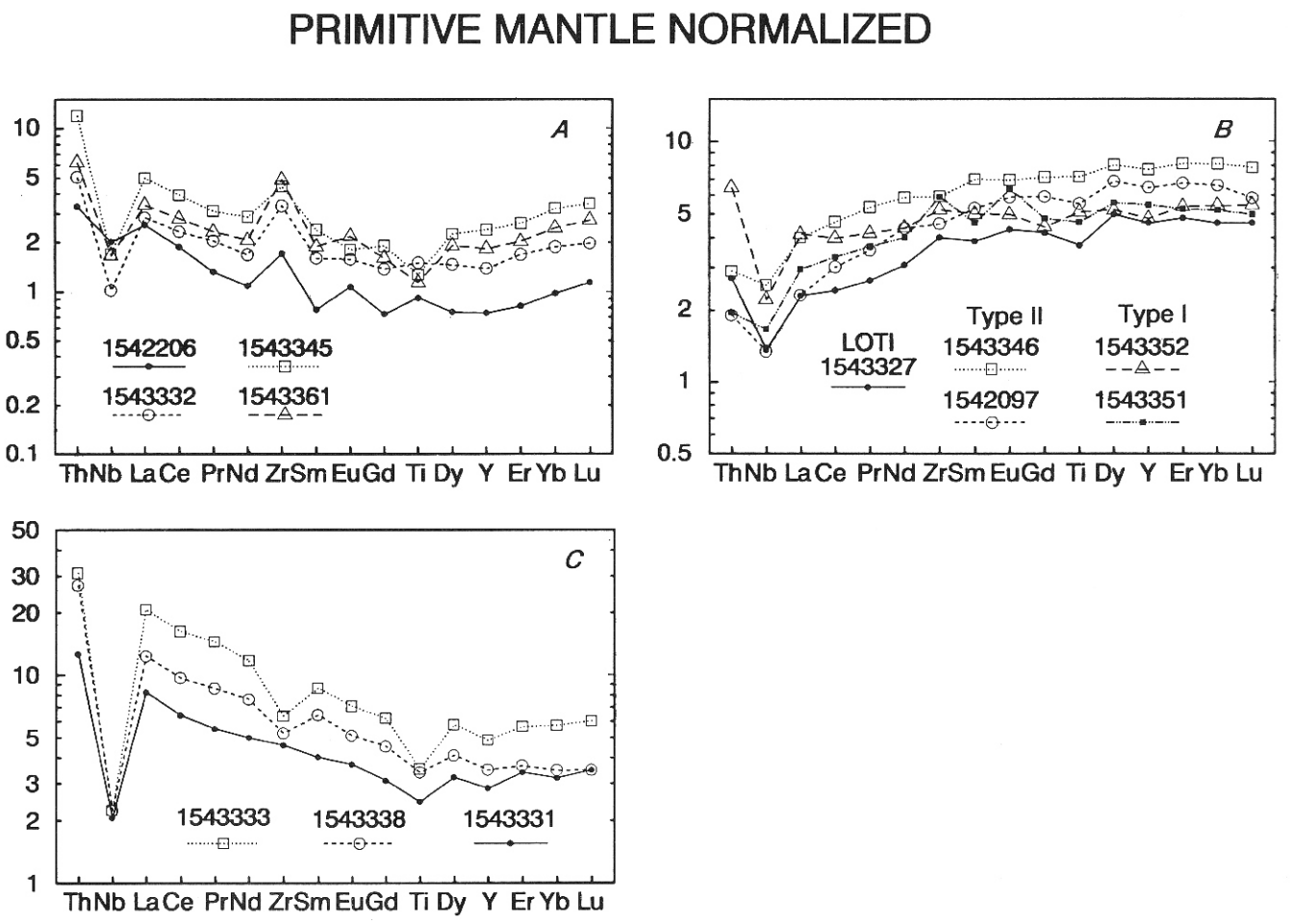

Figure 35. *Primitive mantle normalized extended REE patterns for Lushs Bight Group dykes (A—boninites, B—IAT (type I and II) and LOTI, C—CAB).*

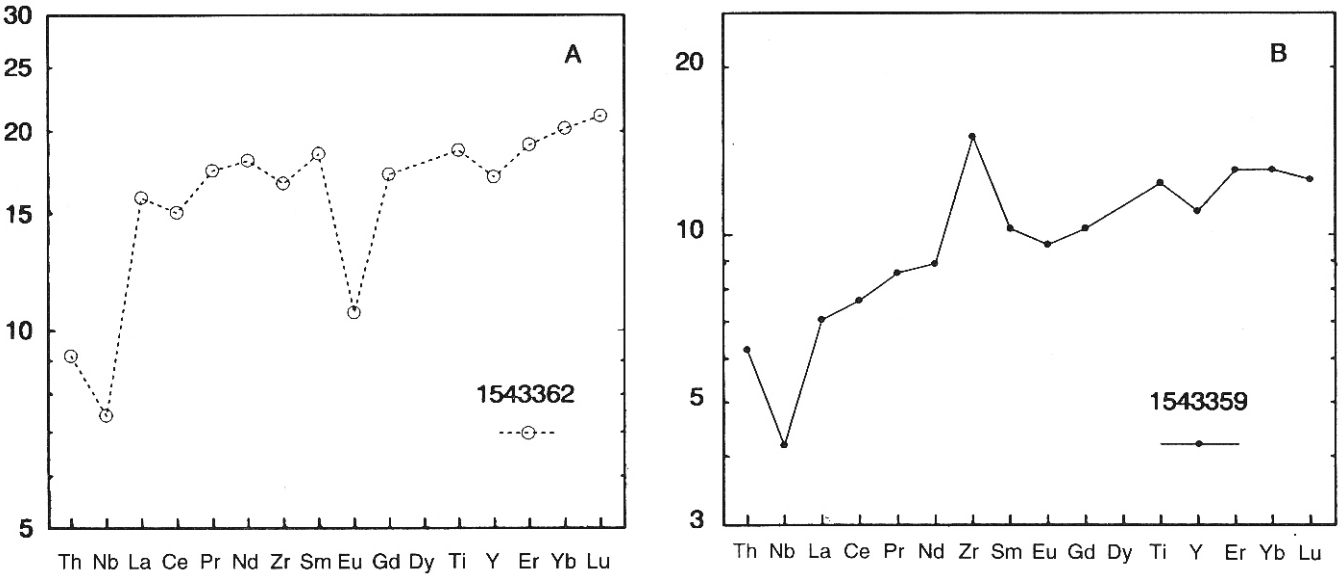

Figure 36. *Primitive mantle extended REE patterns for felsic rocks, Lushs Bight Group (A—felsic volcanic, B—felsite— epidosite dyke).*

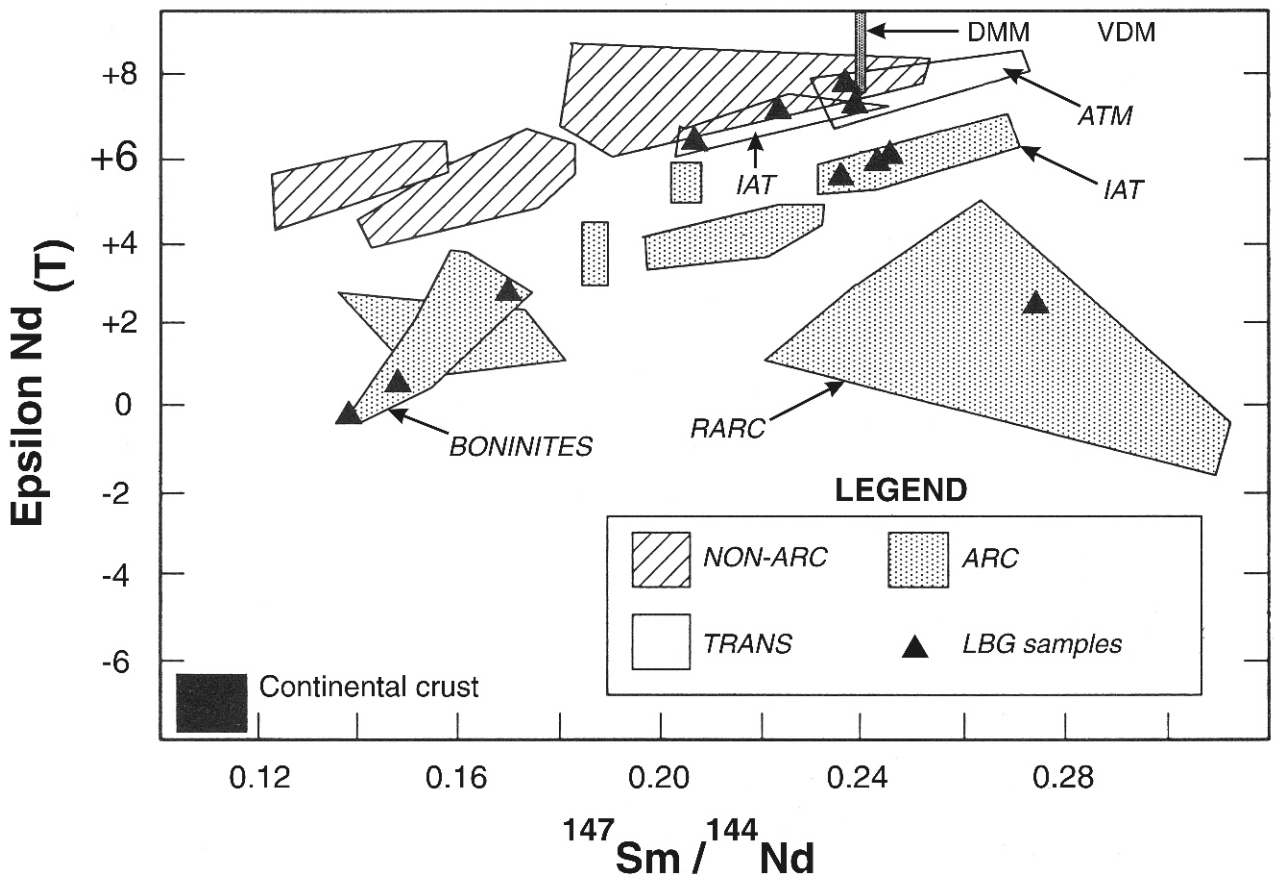

Figure 37. *Sm—Nd isotopic data for the Lushs Bight Group and comparison with other Ordovician Newfoundland volcanic rocks. Non-arc and arc fields based on about 80 isotopic determinations and ICP-MS analyses from volcanic rocks in ophiolites and volcano-sedimentary sequences throughout central Newfoundland (Jenner* et al., *1990; Swinden* et al., *1990). DMM = depleted MORB mantle (based on range for N-MORB today, White, 1985; von Drach* et al., *1986), VDM = very depleted mantle, estimated extreme for depleted mantle. IAT, ATM, BONINITE and RARC fields correspond to our range for island-arc tholeiites, arc-transitional-MORB, boninitic and refractory arc-volcanic rocks. Continental crust field based on average present day value of Nd = -16 and average upper continental crust composition (Taylor and McLennan, 1985).*

There are three major geochemical groups within the Lushs Bight Group that are common to both the lavas and dykes. They are boninites, island-arc tholeiites, and low-Ti tholeiites (LOTI). There are also small groups of non-arc (MORB) lavas and dykes and calc-alkalic (CAB) dykes. Heterogeneities with regard to major, trace and isotopic compositions exist in all of the groups.

All of the geochemical groups show mobility of the LFSE such as K, Na and probably Ba. The non-boninitic rocks show some evidence of major-element mobility, particularly with regard to SiO_2 and FeO*/MgO relative to Al_2O_3. The relative mobility of FeO* and MgO probably causes some scatter and/or change in FeO*/MgO ratios. However, the changes are not, in general, great enough to preclude use of this or similarly based fractionation indicators, especially in light of HFSE heterogeneity in the Lushs Bight Group volcanic rocks. However, the element concentrations and variations observed in the boninites are similar to modern day ones, indicating that they have not undergone significant modification of their major element characteristics. The transition elements (TE), HFSE, Th and REE appear to have been stable or at least behaved coherently for all the geochemical groups. They are used in identifying the tectonic environment of the Lushs Bight Group.

Basalt and basaltic-andesite are the dominant rock types, however, minor felsic rocks (rhyodacite—rhyolite) are present. The boninites are dominantly high-Mg andesites and andesite-basalt with high Cr and Ni and low Ti. In some cases, they may represent primary or primitive mantle-derived melts. The geochemical analogies with modern and ancient boninites suggest that these rocks could have been clinoenstatite-bearing; however, primary minerals and textures have been destroyed. The IAT are

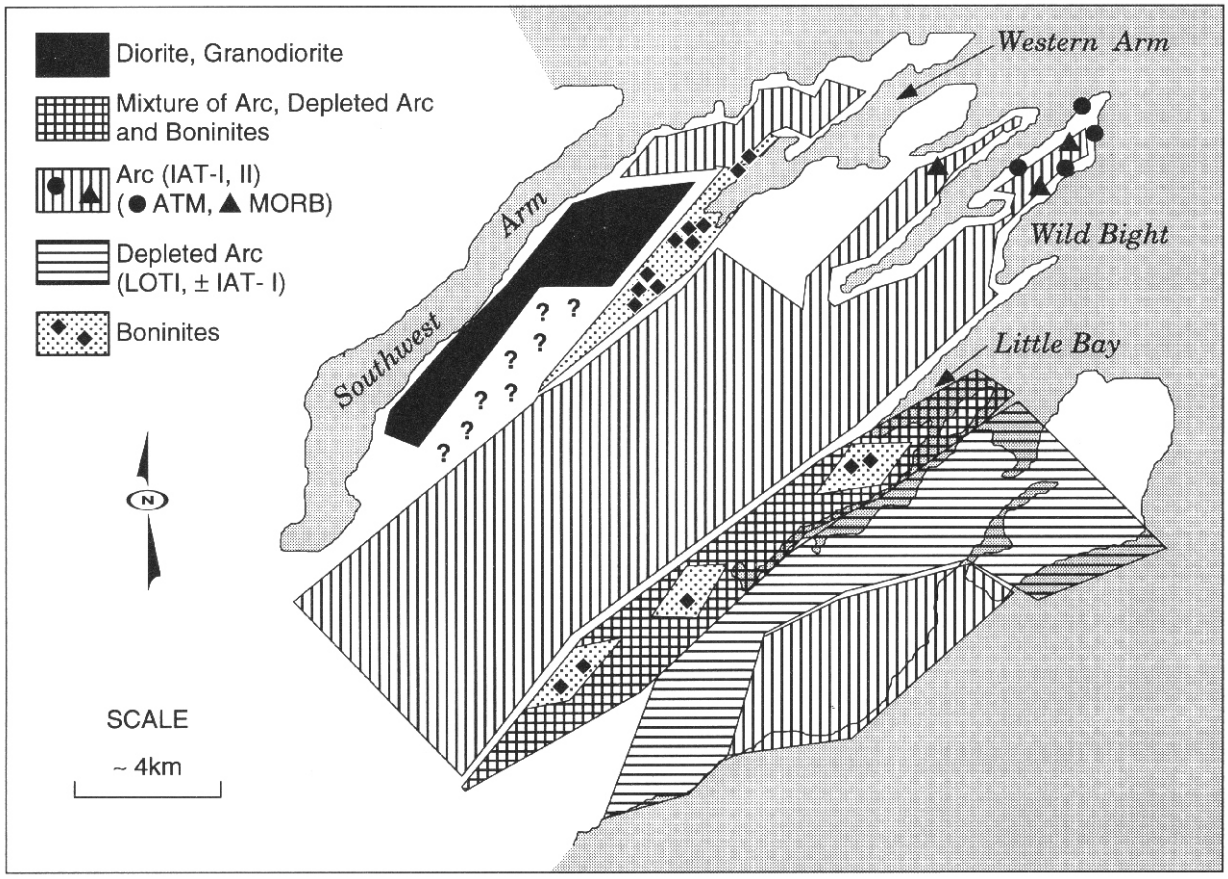

Figure 38. *Schematic map illustrating the distribution of the geochemical groups within the Lushs Bight Group (see text for explanation).*

areally the most extensive geochemical group. They have Ni, Cr and Ti vs Cr, HFSE and REE typical of orogenic environments. The LOTI group is intermediate between the IAT and boninites with respect to Mg# and Ti content. However, the petrogenesis of these rocks seems more clearly linked to the IAT.

Whereas there are marked similarities in chemistry between the lavas and dykes, significant differences are also present. The dykes contain a number of low-Ti and low Mg# rocks, referred to as LOTI-FH and LOTI-F, that are not present in the lavas. A distinct group of dykes (CAB) with calc-alkalic tendencies, primitive magma characteristics (high Mg#, Cr and Ni) and LREE enrichment cut the boninitic lavas south of Western Arm. These dykes could be related to the Cooper's Cove and Colchester plutons, which also intrude the Lushs Bight Group. The rocks are similar to the high-Mg andesites— sanukitoids described by Tatsumi and Ishizaka (1981, 1982) and are interpreted as primary andesitic magmas.

The non-arc or MORB-like rocks are characterized by high TiO_2, by Ti/V ratios > 20, by Nb/Th ratios > 8.2. These are all indicative of a non-arc tectonic environment. The dykes have a wide geographic distribution within the Lushs Bight Group area, whereas the lava (basalt) occurs at the top of the Lushs Bight Group near the contact with the overlying Western Arm Group.

SPATIAL RELATIONSHIPS OF THE GEOCHEMICAL GROUPS

Spatial relationships between the different geochemical groups are illustrated schematically in Figure 38. The geochemical group distribution map was drawn using the following procedures: i) compilation of all available geochemical data, ii) construction of a map showing only lava geochemistry, iii) identification of areas of concentrations of particular geochemical groups of lava, iv) integration of dyke data into the map, and wherever possible, crosscutting relationships between geochemical types was established, and v) comparisons with geochemical data on volcanics in other groups and intrusive bodies. The maps distribution pattern in Figure

38 may include one or more geochemical groups, or parts thereof, because of the spatial component. It should be noted that in general there appears to be no correlation between geochemical grouping and the two metamorphic facies (i.e., main and black, discussed in the section on Structure and Metamorphism) found in the Lushs Bight Group, except for the MORB-like lava at the top of the Lushs Bight Group near the Western Arm Group contact.

Boninitic rocks are restricted to two linear belts, southwest of Western Arm and southwest of Little Bay, respectively (Figure 38). Deformed and undeformed boninitic pillow lavas cut by boninitic dykes form a relatively continuous zone of outcrop in the Western Arm area. Calc-alkalic (CAB) dykes are also extensive in this area. The area indicated by question marks on Figure 38, indicates that insufficient sampling and analytical data are available to enable characterization. In the Little Bay area, boninitic lavas and dykes occur as a discontinuous belt extending from the Little Bay Mine area to Davis Brook. This area consists of fault-bounded blocks of lavas and dykes but the samples from any given block tend to form a consistent geochemical group. Boninitic dykes have not been documented to cut rocks of depleted arc (LOTI) or arc (IAT, ATM, MORB) affinity, although in the sheeted diabase dyke unit north of Lady Pond there are ambiguous intrusive relationships between boninitic and IAT-II dykes. A dyke of LOTI affinity cuts boninites in the Little Bay area. In the Western Arm and Little Bay areas dykes of calc-alkalic and MORB affinity cut the boninites.

The IAT group Types I and II, is referred to as the `arc group'; Types I and II could not be spatially separated. The `arc-group' rocks underlie the central part of the Springdale Peninsula, an area west of Western Arm and an area northeast of Springdale. Arc rocks transitional to MORB (ATM, see Figure 29) and MORB, i.e., lacking a well-defined negative Nb anomaly but with overall low HFSE and REE abundances, are included in this group because of the high degree of heterogeneity in Nb and Th for a given Y content (see Figure 29). They occur in abundance in the Wild Bight area, but it is known that these rocks are more widespread; however, further definition is hampered by the lack of detailed chemical sampling and analytical data (especially for Th, Nb, REE).

The LOTI group and some of the most depleted IAT-I group were combined to form the `depleted arc' group. Depleted arc rocks intruded by `arc-group' and MORB-affinity dykes, constitute most of the eastern outcrop area of the Lushs Bight Group. Fault-bounded blocks of depleted arc volcanic rocks are also found structurally interleaved with boninitic and arc rocks in a linear belt between Little Bay—Davis Brook (cross-hatched area on Figure 38). Present outcrop distribution of the depleted arc rocks is almost certainly controlled by thrust faults (A. Szybinski, personal communication, 1990), with the `depleted arc' volcanic rocks thrust over the `arc' rocks.

A summary diagram of the probable stratigraphic, geochemical and isotopic relationships within the Lushs Bight Group is given in Figure 39. Boninitic volcanism appears to have been the first event in the evolution of the Lushs Bight Group. Subsequent volcanism involved less refractory mantle sources and gave rise to the `depleted arc' (dominantly the LOTI group) and `arc group' (IAT, ATM, MORB).

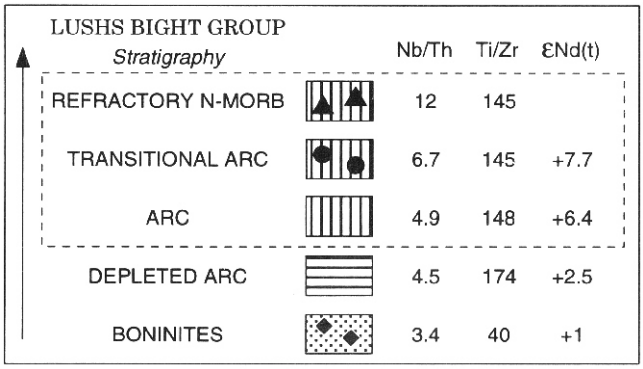

Figure 39. *Summary diagram linking stratigraphic, geochemical and isotopic characteristics of the Lushs Bight Group. Note that symbols and patterns are keyed to Figure 38 (transitional—1542024; ARC—average of 1542249, 1542036, 1542266, 1542267, 1542151, 1542004; depleted ARC—1542116, and boninites—average of 1542118, 1542206, 1543361).*

The stratigraphic relationships of boninites in the Lushs Bight Group differs from those in the Betts Cove Complex (Coish *et al.*, 1982; Coish, 1977). There boninitic pillow lavas are intimately associated with other arc volcanic rocks, and are overlain by non-arc MORB and non-arc transitional tholeiites of the Snooks Arm Group (Jenner and Fryer, 1980; Jenner *et al.*, 1990). Volcanism in the Betts Cove Complex is interpreted to record arc-rifting and back-arc basin formation (Coish *et al.*, 1982; Crawford *et al.*, 1981; Swinden *et al.*, 1989). In contrast, boninites of the Lushs Bight Group are overlain by extensive island-arc tholeiites that are in turn overlain by volcanic rocks of back-arc affinity. There is no record of active boninitic volcanism during the arc to back-arc formation in the Lushs Bight Group. The geochemical evolution of the Lushs Bight Group is shown schematically in Figure 40. The occurrence of boninites in the Lushs Bight Group is consistent with petrogenetic models proposed by Cameron *et al.* (1979), Meijer (1980), and

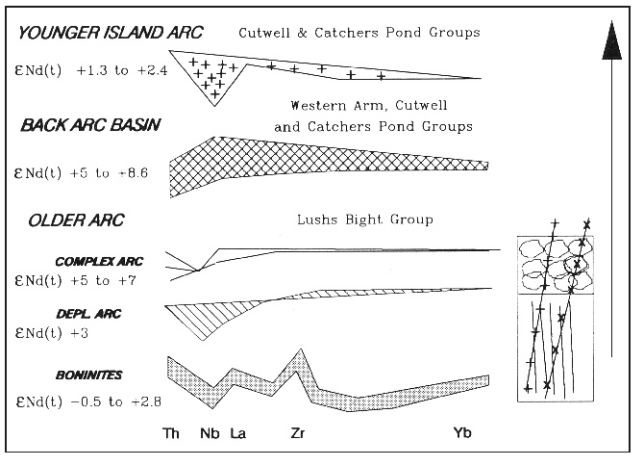

Figure 40. *Schematic diagram summarizing tectonic, stratigraphic, geochemical and isotopic features of ophiolitic and volcano-sedimentary groups in western Notre Dame Bay. Arrow on the right side indicates way-up. Inset in lower right corner illustrates ophiolite stratigraphy of the Lushs Bight Group, cut by dykes indicating possible link to the younger island-arc groups (+), and to the back-arc basin groups (x). Note that crosscutting relationships between the CAB and MORB dyke `types' were not observed.*

Bloomer and Hawkins (1987), which have boninitic volcanism accompanying the earliest stages of island-arc formation.

COLCHESTER AND COOPER'S COVE PLUTONS

The Colchester and Cooper's Cove plutons are composite bodies, ranging in composition from diorite to granite. Major- and trace-element data for representative samples from the plutons are given in Appendix 2, Table 2-4. The geochemical database for these plutons is small, and therefore, any interpretation of tectonic environment is tenuous.

These plutons range in silica content from 54 to 78 percent, but are dominated by rocks having intermediate silica contents (56 to 63 percent). Metaluminous tonalites, minor quartz diorites and granodiorites (Figures 41 and 42) are the most common rock types (LeMaitre, 1989; Kosinowski, 1982; Debon and LeFort, 1983). The plutons are extremely low-K and generally plot in the calc-alkaline field with a minor transgression into the tholeiitic field (Figure 43) (Jensen, 1976; Irving and Baragar, 1971). They are classified as volcanic-arc granites (Figure 44) on the trace-element discrimination plot of Pearce *et al.* (1984a). All of the samples show some degree of light

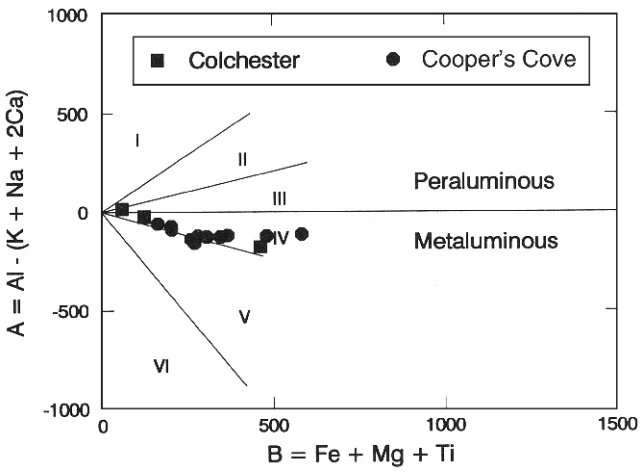

Figure 41. *Metaluminous vs peraluminous plot for the Colchester and Cooper's Cove plutons.*

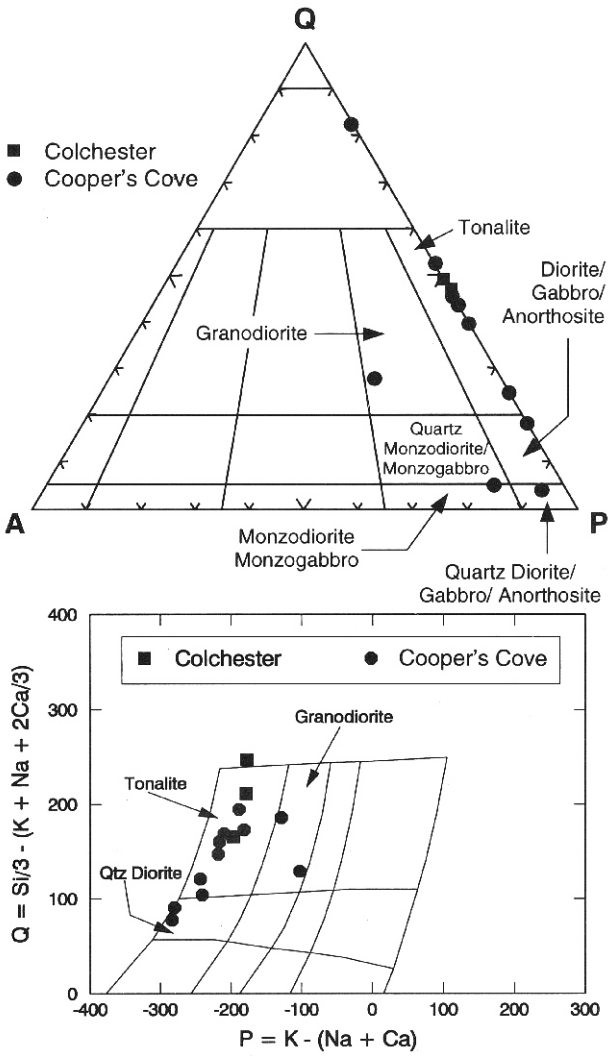

Figure 42. *Rock classification plots for Colchester and Cooper's Cove plutons.*

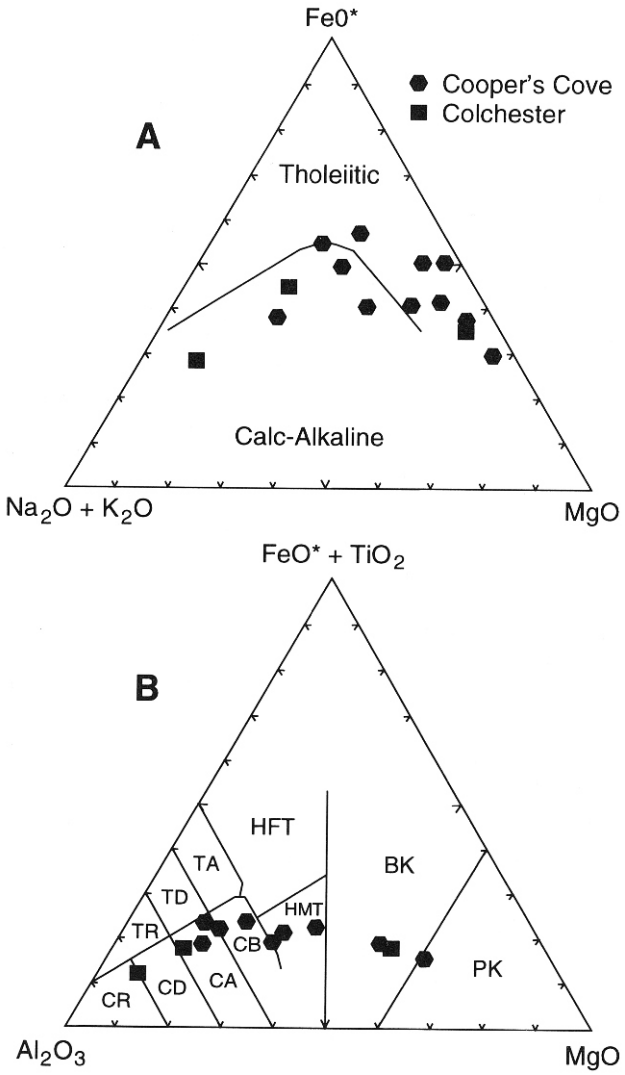

Figure 43. *Ternary plots depicting the tectonic classification of the Colchester and Cooper's Cove plutons.*

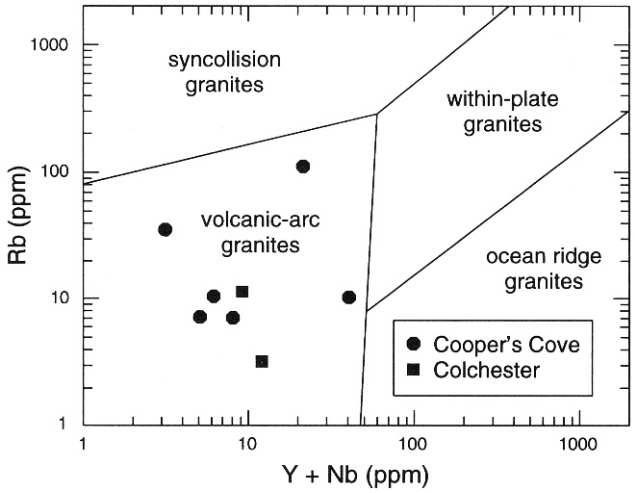

Figure 44. *Rb vs Y + Nb discriminant diagram for the Colchester and Cooper's Cove plutons.*

REE enrichment (Figure 45). The samples having positive Eu-anomalies are probably cumulate in origin. All of the plutonic rocks are characterized by negative Nb-anomalies, consistent with their definition as volcanic-arc granites. The patterns in the plutons show more similarity with the late calc-alkaline dykes than with the felsic dyke (IAT-like) considered part of the Lushs Bight Group.

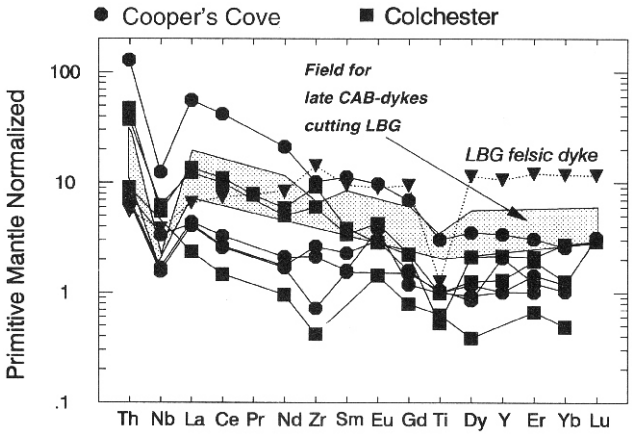

Figure 45. *Primitive mantle normalized plot for plutonic rocks of the Colchester and Cooper's Cove plutons (Samples 1542226, 1542229, 1542271, 1542272, 1542275, 1542311 and 1543324). Comparison field and pattern for later calc-alkalic dykes and a Lushs Bight Group felsite—epidosite dyke overlapped. Normalizing values after Hofmann (1988).*

The origin of the plutonic rocks is not clear. Some of the granodiorites show close compositional affinities with the Toulumme Intrusive Series of the Sierra Nevada Batholith (see Hess, 1989, page 170). However, the low K content suggests more similarity with intra-oceanic arcs. The age of the plutons (~465 Ma, Szybinski, 1995) and the extremely low epsilon Nd in some of these rocks (~ -8 to -10) (G. Jenner, unpublished data, 1992), suggest they are post-collisional granites derived from a K-poor but time-integrated old source. The age of the plutonism makes any obvious correlation with active subduction and with the Lushs Bight Group difficult.